UNIVERSITY OF ALGARVE/UNIVERSIDADE DO ALGARVE

EVALUATION OF SCHIFF BASES AND ITS METAL COMPLEXES WITH POTENTIAL THERAPEUTIC APPLICATIONS

ISRAEL ALEMAYEHU TEKAMO

Thesis/Dissertação

Mestrado Erasmus Mundus em Inovação Química e Regulamentação

(Erasmus Mundus Master in Chemical Innovation and Regulation)

Main Supervisor: Dr. Isabel Correia

Co-supervisor: Prof. Isabel Cavaco

October 2019

2019 Israel Alemayehu Tekamo Evaluation of Schiff bases and its metal complexes with potential therapeutic applications

UAlg UNIVERSIDADE DO ALGARVE

UNIVERSITAT DE BARCELONA

ALMA MATER STUDIORUM UNIVERSITÀ DI BOLOGNA

HERIOT WATT UNIVERSITY

UNIVERSIDADE DO ALGARVE

Israel Alemayehu Tekamo

Evaluation of Schiff bases and its metal complexes with potential therapeutic applications

October 2019

Evaluation of Schiff bases and its metal complexes with potential therapeutic applications

Declaration of Authorship

I declare that I am the author of this work, which is original. The work cites other authors and works, which are adequately referred in the text and are listed in the bibliography.

Israel Alemayehu Tekamo

Dedication

To my parents,

Alemayehu Tekamo Gosoma

and

Tsehaynesh Agena Ataro

Your support and drive are what has made me who I am today.

Acknowledgements

First, I would like to thank the almighty God for giving me the strength to complete my study. Without his blessings, this accomplishment would not have been possible.

The achievement and outcome of this project required a lot of guidance and assistance from many people and I am extremely privileged to have got this all along the completion of my project. All that I have done is only due to such supervision and assistance and I would not forget to thank them all.

My first and foremost appreciation and deepest sense of gratitude goes to my esteemed supervisor Dr. Isabel Correia. I would like to thank her for constant and warm encouragement, thoughtful guidance, insightful decision, critical comments and patience in reading, reviewing and correcting this thesis manuscript.

I am also thankful to Professor João Costa Pessoa for allowing me to do this work in his laboratory. I also would like to thank Dr. Samuel Silvestre for the cytotoxicity studies and Dr. Adriana Santos for the microbiology from the University of Coimbra for their help with these specific tests and techniques performed during this work. Their expertise and enlightenments in their respective field of research provided me with the necessary tools for the conclusion of this work.

I owe special acknowledgement and appreciation to Patrique Nunes and Nadia Ribeiro for their kind assistance during my laboratory works from the beginning to the end. I would like to appreciate their personalities and expertise they shared me at CQE.

I would like to offer my sincere thanks to Professor Isabel Cavaco from University of Algarve and Professor Daniel Sainz from University of Barcelona for their supports in CHIR program. I also would like to acknowledge University of Algarve, Bologna University, Barcelona University, Heriot Watt University, Instituto Superior Técnico and Centro de Química Estrutural.

My sincere gratitude is also to European commission for financial support to attend this program. I would like to thank Dr. Nataliya Butenko and Dr. Dina Jesus from university of Algarve for lending their kind cooperation in matters we request with great motivation and enthusiasm.

Finally, I would like to thank my families and kids for the love they shared and for the patience they showed me during this study and tremendous contributions in my life.

Abstract

Metal-based drugs have drawn significant attention over the past few decades due to their advanced properties and benefits in biomedical therapeutic and diagnostic systems. In the current work two Schiff bases, 4-methyl-2,6-bis-(pyridin-2-yl-hydrazonomethyl)-phenol (**L1)**, and methyl-phenol-di-S-methyl dithiocarbazate (**L2)**, and their corresponding zinc complexes, $[Zn_2(L1)(OAc)_3]$ **(C1**) and $[Zn_2(L2)(OAc)]$ (**C2**) (OAc: CH_3COO^-) were synthesized. All compounds were characterized by elemental analyses, FTIR, UV–Vis and NMR spectroscopies and ESI-MS spectrometry. The stability of the compounds was evaluated under physiological conditions (5 % DMSO and 95 % PBS, pH 7.4). The interaction of Schiff bases and their corresponding Zn(II) complexes with biomolecules namely, bovine serum albumin (BSA) and *calf thymus* DNA (ctDNA) was investigated using UV-Vis, circular dichroism (CD) and fluorescence spectroscopies under physiological pH and 298 K. Fluorescence quenching of BSA upon interaction with the compounds was analysed using the Stern-Volmer formalism which revealed moderate to strong binding to serum albumin with binding constant values of $K_B=2.36x10^3$ and $2.38x10^5 M^{-1}$, for **C1** and **C2** respectively. These results reveal good binding propensity in comparison with the ligands. Changes in the secondary structure of BSA are imposed by the Schiff base ligands and Zn(II) complexes as revealed by CD spectroscopy. Additionally, hypochromicity in the UV-Vis absorption spectra of the complexes upon addition of BSA further corroborates interaction between the protein and the complex. The complexes were tested for their DNA binding ability by UV-Vis and CD spectroscopy and the results indicate that there is interaction between the complexes and DNA where **C1** has better binding tendency toward DNA than **C2**. Cytotoxic activity of **L1** and **L2** studied with several tumour cell lines (Caco-2, MCF-7 and PC-3) and normal cell, NHDF, showed that the compounds are cytotoxic to all cell lines tested, without selectivity towards cancer cells. Overall, the IC_{50} values are comparable with the ones obtained for the positive control, fluorouracil. The two ligands and one complex were tested against several strains of bacteria and fungi and promising results were obtained, where **L1** is active against *L. monocytogenes*, **L2** is active against *K. pneumoniae*, *A. baumannii* and *S. aureus* and **C1** against *L. monocytogenes* and *S. aureus*. **L2** showed better activity against the tested microorganisms compared to **L1** and the metal complex.

Keywords: Schiff bases, Zn(II) complexes, cytotoxicity, albumin, DNA.

Resumo

Nas últimas décadas os fármacos à base de metais de transição têm sido alvo de grande atenção devido às suas propriedades e benefícios em sistemas terapêuticos e de diagnóstico. Neste trabalho, sintetizaram-se duas bases Schiff, 4-metil-2,6-bis-(piridina-2-il-hidrazonometil)-fenol (**L1)**, e ditiocarbazato de metil-fenol-di-S-metilo (**L2**), e dois complexos, $[Zn_2(L1)(OAc)_3]$ (**C1)**, e $[Zn_2(L2)(OAc)]$ (**C2**). Os compostos foram caracterizados por análise elementar, espectroscopias de FTIR, UV-Vis, RMN e por espectrometria de massa. A estabilidade dos compostos foi avaliada em condições fisiológicas (5% de DMSO e 95% de PBS, pH 7.4). A interação das bases Schiff e seus complexos de Zn(II) com biomoléculas, nomeadamente albumina sérica bovina (BSA) e DNA do timo de bezerro (ctDNA), foi investigada usando espectroscopia de UV-Vis, dicroísmo circular (DC) e fluorescência, a pH fisiológico e 298 K. Analisou-se a extinção da fluorescência da BSA após interação com os compostos usando o formalismo de Stern-Volmer, que revelou ligação moderada a forte à albumina sérica, tendo sido obtidos valores de constantes de ligação de $2.36x10^3$ e $2.38x10^5$ M^{-1}, para **C1** e **C2**, respectivamente. Estes resultados revelam maior afinidade dos complexos pela BSA, quando comparados com os ligandos. Alterações na estrutura secundária da BSA são impostas pelos complexos de Zn(II), conforme revelado por espectroscopia de DC. Adicionalmente, a hipocromicidade observada nos espectros de absorção no UV-Vis, após a adição de BSA, corrobora a interação entre a proteína e os complexos. Os complexos foram testados quanto à sua capacidade de ligação ao DNA recorrendo à espectroscopia UV-Vis e DC, e os resultados indicam que há interação entre os complexos e o DNA, e que **C1** tem mais afinidade pelo DNA do que **C2**. A atividade citotóxica de **L1** e **L2**, estudada em várias linhas tumorais (Caco-2, MCF-7 e PC-3) e numa linha normal (NHDF), mostraram que os compostos são citotóxicos para todas as linhas celulares testadas, sem seletividade para as células cancerígenas. No geral, os valores de IC_{50} são comparáveis aos obtidos para o controlo positivo, fluorouracil. Os ligandos e **C1** foram testados contra várias estirpes de bactérias e fungos e foram obtidos resultados promissores. **L1** é ativo contra *L. Monocytogenes*, **L2** é ativo contra *K. pneumoniae*, *A. baumannii* e *S. aureus* e **C1** contra *L. monocytogenes* e *S. aureus*. **L2** foi o que apresentou maior atividade contra os microorganismos testados, quando comparado com **L1** e **C1**.

Table of Contents

Index of Figures

Index of Tables

Index of Schemes

Symbols and abbreviations

DNA → Deoxyribonucleic acid

(n→π*) → Electronic transition from the n orbital to the π* orbital

(π→π*) → Electronic transition from the π orbital to the π* orbital

^{13}C NMR → Carbon 13 nuclear magnetic resonance

^{1}H NMR → Proton nuclear magnetic resonance

COSY → Homonuclear correlation spectroscopy (COSY)

DEPT → Distortion less enhancement by polarization transfer

DMSO → Dimethyl sulfoxide

ESI-MS → Electrospray Ionization Mass Spectrometry

FTIR → Fourier Transform Infra-Red Spectroscopy

*ct*DNA → *Calf thymus* DNA

HMBC → Heteronuclear multiple-bond correlation spectroscopy

IC_{50} → Half-inhibitory concentration

m/z → mass/ charge

MeOH → Methanol

MilliQ → Double deionized water

PBS → Phosphate Buffered Saline

Smdt → S-methyl dithiocarbazate

UV-Vis → Ultra-Violet-Visible Spectroscopy

δ → chemical shift

ε → extinction coefficient

λ_{em} → Fluorescence emission wavelength

λ_{ex} → excitation wavelength

λ_{max} → maximum wavelength

ν → vibration frequency

1. Introduction

The discovery of novel active compounds with new mechanisms of action, higher efficacy and improved selectivity is a matter of urgency to multi drug resistance and toxicity problems associated with many therapeutic drugs [**1**]**.** Great attention has been given to transition metal complexes and extensive biological effects have been found for many of them [**2**]. One of the first therapeutic metallodrugs was salvarsan (**Fig. 1a**), an arsenic-based antimicrobial agent developed by Paul Ehrlich for the treatment of syphilis. With the addition of mercury and bismuth, salvarsan remained the standard remedy for syphilis until it was replaced by penicillin after World War II. Salvarsan is regarded as the birth of modern chemotherapy and often cited as the beginning of modern research and development of metallodrugs. In 1965, the star of the field, the anticancer agent cisplatin, was discovered by Barnett Rosenberg and Loretta Van Camp at Michigan State University [**3**]. This platinum-based anticancer drug (**Fig. 1b**) has played a crucial role in Medicinal Chemistry. Complexes with other metal ions like titanium and ruthenium are also being explored with some success but none of them have been used in the clinic yet [**2**,**4**].

Despite the achievements in the metal-based drugs, especially those of platinum, they are still associated with many drawbacks such as general toxicity, nonspecific targeting and acquired drug resistance, which has stimulated researchers to seek and develop more effective, less toxic, and target-specific metal-based drugs [**5**]. Complexes based on essential transition metals, such as Co(II), Ni(II), Cu(II) and Zn(II) have been found interesting in this respect. These metal ions are biocompatible, endogenous and they are present in biological systems [**4**,**5**]. They are nowadays present in several inorganic drugs used against a variety of diseases [**4**].

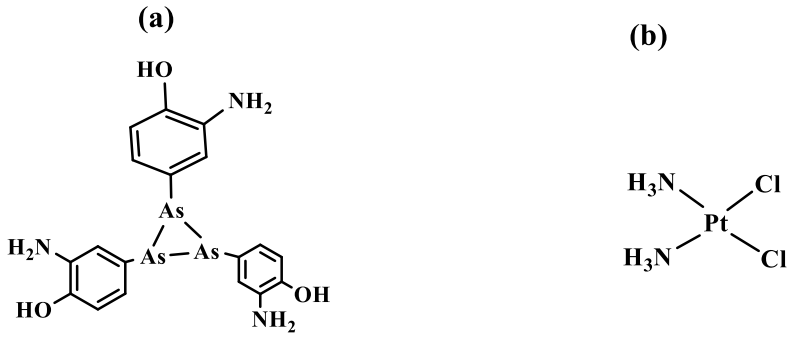

Figure 1 Salvarsan (**a**) and cisplatin (**b**) metallodrugs **[**3**]**.

Transition metal complexes possess several advantages that make them attractive alternatives to small organic molecules for the development of therapeutic agents. They can adopt numerous geometries, including square-planar, square-pyramidal, trigonal-bipyramidal and octahedral, depending on the coordination number of the metal ion. Many of these geometries are unavailable to purely organic molecules, which are limited to linear, trigonal planar or tetrahedral shapes because carbon cannot exceed a coordination number of four. The diversity of molecular structures afforded by transition metal complexes may therefore allow them to sample regions of the chemical space that are inaccessible to organic molecules. Moreover, metal complexes can undergo redox reactions and ligand-exchange reactions inside the body, allowing for unique mechanisms of action to take place [**6**]. In general, because of the intrinsic nature of their centres, characteristic coordination modes, accessible redox states and kinetic properties allow metal complexes to offer potential advantages over organic agents alone [**2**]. However, the role of the ligands in the metal complex is also very important. For example, they control the reactivity of the metal and determine the nature of interactions involved in the recognition of biological target sites such as deoxyribonucleic acid (DNA), enzymes and protein receptors. Therefore, the choice of ligands for the formation of metal-based drugs is crucial. As a result, a great expansion of research in the coordination chemistry of sulphur and nitrogen containing ligands such as Schiff bases and phenanthroline derivatives has taken place during recent years [**7**,**8**].

1.1 Schiff-base ligands

Schiff-base ligands and corresponding metal complexes have received much attention in recent years due to their wide use as dyes and pigments, catalysts, intermediates in organic synthesis, polymer stabilizers and due to their broad range of biological activities, including anti-fungal, anti-bacterial, anti-malarial, anti-proliferative, anti-inflammatory, anti-viral, and anti-pyretic properties [**9-12**]. Schiff bases are aldehyde or ketone like compounds in which the carbonyl group is replaced by an imine or azomethine group. It contains a carbon-nitrogen double bond with the nitrogen atom connected to an aryl or alkyl group but not hydrogen.

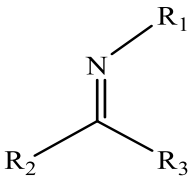

Schiff Base

Figure 2 The structure of a Schiff base.

Schiff bases are of general formula $R^1N=CR^2R^3$, where R^1 is a phenyl or alkyl group which gives the Schiff base its stability [**13**]. Although the formation of Schiff bases is reversible, due to the hydrolysis of the imine under certain conditions, it is still straight-forward for the reaction to succeed. It is still unknown why some types of Schiff bases are stable in the presence of water even in acidic solution, while others are very sensitive to water and easily hydrolyse back to aldehyde (or ketone) and amine.

To overcome this potential hydrolysis, the reaction of Schiff bases should be undertaken under dry solvent conditions or using some additional procedure to remove the side product, water. The lone pair on the nitrogen atom of the imine can supply electrons, which enable the formation of a proper donor bond to a metal ion for complexation to occur. Many Schiff bases have a second functional group, normally OH and SH groups or another N atom, which are near the imine group. These functional groups can allow the formation of five or six membered chelate rings when coordinated with different metal ions.

1.2 History of Schiff-bases

Schiff bases are named after Hugo (Ugo) Schiff (1834-1915), a German chemist. He discovered Schiff bases in 1864 and other imines and was responsible for research into aldehydes and had the Schiff test named after him. Fuchsine (shown in **Figure 3**) was studied by Schiff as a Schiff reagent in 1866, which was apparently widely used during the last decades of the 19th century for industrial dyes.

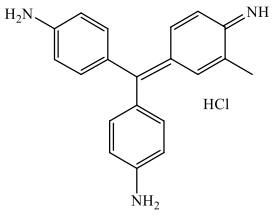

Fuchsine

Figure 3 Structure of fuchsine.

A well-known Schiff base is salen [**14**], which stands for *N*,*N*′-ethylenebis(salicylaldimine) (**Figure 4**), a bi-functional and tetradentate (ONNO) ligand. Several asymmetric salen type Schiff bases were reported by R. Atkins [**15**] in 1985, who suggested a more general term for these tetradentate (ONNO) ligands: salen-type. The 2-hydroxybenzaldehyde is a suitable building block due to the possible substitution patterns of the aromatic ring. Once the imine bond is formed from primary amine and aldehyde, this orientation of salen-type Schiff bases will form a more stable six-member ring when binding to metal ions.

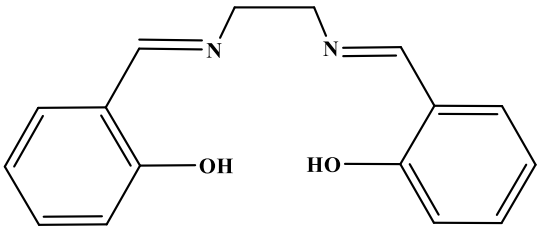

Salen ligand

Figure 4 Typical structure of salen-type ligands.

1.3 Synthesis of Schiff-base ligands

The Schiff base reaction is a reversible, usually acid-catalysed condensation between a primary amine (not ammonia) and either an aldehyde or a ketone. The Schiff base is the nitrogen analogue of an aldehyde or ketone, in which the carbonyl group is replaced by an imine group (C=N-R), which is shown in **Scheme 1** where R may be an alkyl or an aryl group.

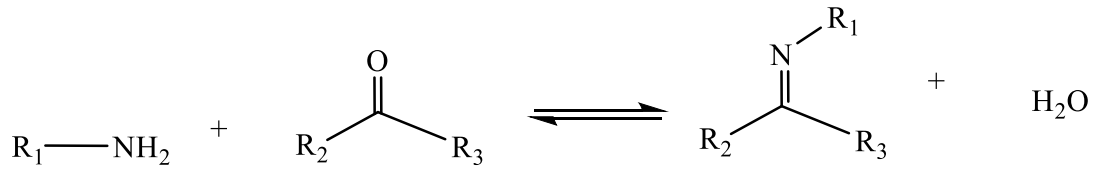

Primary amine Aldehyde or Ketone Schiff base Water

Scheme 1 The synthesis of Schiff Bases.

Schiff bases, which contain aryl substituents, are more stable and more easily synthesized than those containing alkyl substituents. This means that Schiff bases of aliphatic aldehydes are relatively unstable, and they readily undergo polymerisation in comparison to products from conjugation of aromatic aldehydes [**16-20**]. Typically, the formation of Schiff bases from aldehydes or ketones requires a protic solvent sufficiently dry to prevent potential hydrolysis of the newly formed imine bond. The formation is generally undertaken under acid or base

catalysis, or upon heating. The completion of imine formation is controlled by the separation of the product or removal of water, or both.

1.4 Mechanism of Schiff bases formation

The mechanism of Schiff base formation, as shown in **Scheme 2**, involves a nucleophilic addition to the carbonyl group. In the Schiff base formation, the nucleophile is the primary amine. In the first part of the mechanism, the lone pair of electrons in the amine nitrogen attacks the aldehyde or ketone to give an unstable addition compound called a carbinolamine [**21**]. A 1,3-hydrogen shift follows, which facilitates the loss of water by either acid or base catalysis. Since the carbinolamine is an alcohol, it undergoes acid catalysed dehydration.

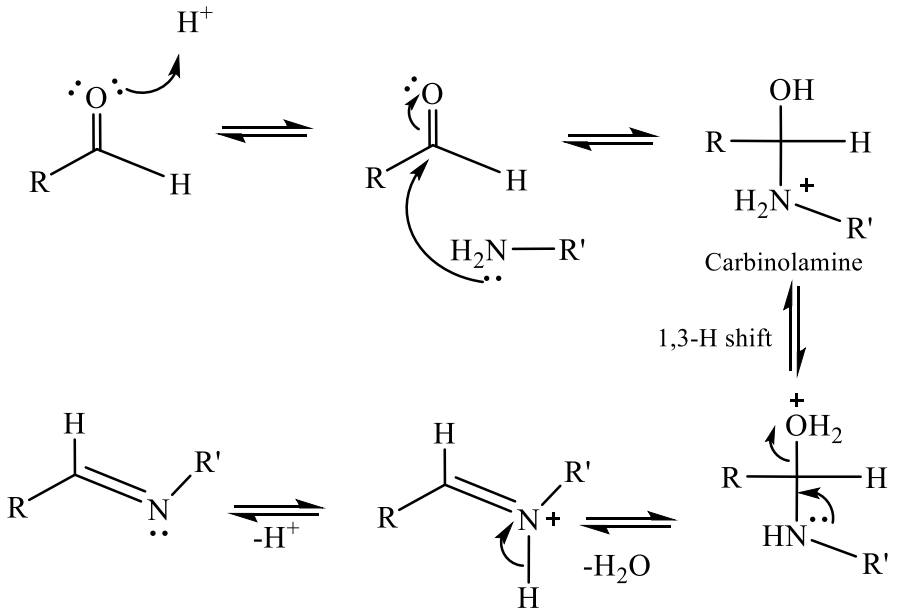

Scheme 2 Mechanism of acid catalysed Schiff base formation.

The rate-determining step of Schiff base formation is the dehydration of carbinolamine, and that is the reason why the reaction is catalyzed by acids or Lewis acids. But the concentration of acid present for the catalysis cannot be too high as amines are basic compounds. If the amine is deprotonated and becomes non-nucleophilic, equilibrium is pulled to the left and the carbinolamine will go back to aldehyde or ketone and primary amine.

Base catalysis is also used for the dehydration of carbinolamines. The reaction of elimination is analogous to the E2 elimination of alkyl halides. Schiff base formation can be divided into two steps through an anionic intermediate, *i.e.* addition followed by elimination. Generally, the geometry of the imine double bond adopts a *trans* orientation, which limits steric interactions of the bulkier R and R' groups, [**22**].

1.5 Compartmental Schiff base ligands

The chemistry of phenoxo compounds has a great interest in the design of compartmental ligands to study the interaction in polynuclear metal complexes. Compartmental ligands contain two adjacent, similar to dissimilar compartments, which can coordinate two identical or different metal ions in proximity as shown in F**igure 5**. The donor groups of these ligands provide a significant diversification of the coordination sites making them good candidates for metal ion complexation and for mimicking biological systems.

The synthesis of metal complexes using such dinucleating ligands has spurred interest due to their potential applications found in various modern research fields including bioinorganic chemistry, among others [23]. Among various kinds of dinucleating ligands, the phenol-based compartmental ligands of the "end-off" type, possessing two chelating arms attached to the 2- and 6-positions of the phenol ring have attracted a great number of researchers [24]. This is due to the key role played by the phenolic group which has many useful electronic and structural characteristics such as: (i) charge as function of pH values; (ii) bridging capability, often the phenolic donor atom binds two metal centres in proximity; (iii) the benzene ring allows a great synthetic flexibility.

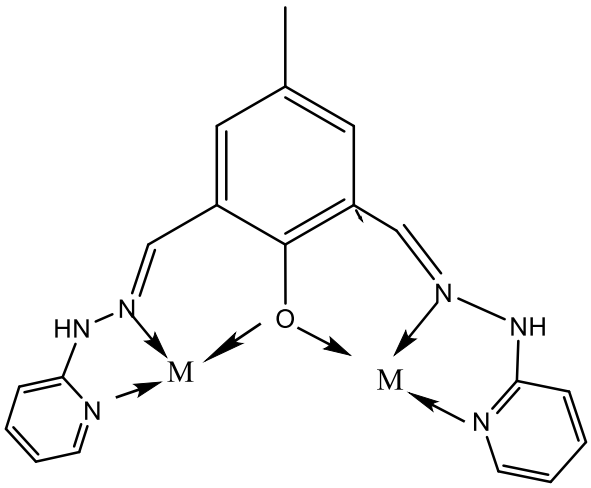

Figure 5 Compartmental symmetrical ligand.

1.6 Schiff-base metal complexation

1.6.1 Overview

Schiff bases are very efficient ligands. The presence of the lone pair of electrons on the nitrogen atom of the imine bond means that they can be donated to the appropriated metal ion. Many

Schiff bases have a second or even third functional group, such as an OH, SH and nitrogen atoms from heterocyclic rings, *e.g.* pyridine or imidazole rings. This electron donation, in conjunction with a functional group, implies that a vast number of transition metal complexes could be prepared. From recent reviews, large numbers of Schiff base complexes have been used in catalysis [**12**], polymer supported in oxidations [**11**], biological applications [**10**], and so on.

1.6.2 Zn(II) Schiff-base complexes

Zinc occurs in low amounts in nature, but, large amounts of zinc ores have been found in the Earth's crust [**25**]. Zinc is a late first row transition metal which has an electronic configuration of [Ar]3d^{10}4s^2 and is a member of group 12 of the periodic table. The chemistry of zinc is controlled by the +2 oxidation state. When Zn is formed in this state, the outer shell *s*-electrons are lost, which yields a bare zinc ion with electronic configuration [Ar]3$d^{10.}$ The full *d*-orbitals imply that Zn(II) complexes are diamagnetic and usually colourless. It also means that the coordination complexes of Zn(II) ions do not have a ligand field stabilisation effect. The stereo-chemistries of these species are determined by considerations of electrostatic forces, covalent bonding forces and the size of the metal ion [**26**].

Zinc Schiff base complexes are well known in coordination chemistry, although not in such large numbers as reported for copper and nickel derivatives. The Zn(II) ion is dominated by either four-, five- or six-coordinate geometry with the four- and five-coordinate geometries being the most common [**26**]. Examples of high/low coordination numbers for Zn^{2+} ions are rare, but still can be found. Sun and co-workers [**27**] reported a pentadentate Schiff base ligand in 2006 and established the Zn(II) complex was seven-coordinate with a pentadentate N_3O_2 Schiff base ligand and two remaining coordination sites occupied by donor solvent molecules. Chisholm and co-workers synthesized a three-coordinate monomeric Zn(II) Schiff base complex in 2001 [**28**]. Six-coordinated Zn(II) Schiff bases complexes are much more common than either the seven- or three-coordinate, Yang and co-workers reported a six-coordinated Zn(II) complex by two N,N'O-tridentate Schiff base ligands, resulting in a slight distorted *trans*-ZnO_2N_4 octahedral coordination for the metal ion [**29**].

Although Zn(II) Schiff bases complexes showed lower catalytic activity (e.g. Zn(II) Schiff base complexes achieved low activity for the decomposition of hydrogen peroxide (H_2O_2) [**30**] than complexes of other metal ions (Ni, Co, Mn or Cu), it showed a wide range of bio-applications

as reviewed by Anand [**10**]. The interaction of a Zn(II) Schiff base complex with DNA was reported by Kumaran and co-workers [**31**]. It was investigated with *in silico* methods and suggested that it could bind DNA though the minor groove and have high activity on anti-bacterial and antifungal testing.

1.7 Biological screening

The physical and chemical properties of compounds determine their biological activities. For example, the rate of absorption, distribution, metabolism and excretion (ADME) of drugs are critical parameters in determining their pharmacokinetics properties. This means that the level of efficacy and toxicity of the drug depends on its concentration at the site of action [**32, 33**]. This, in turn, depends on the solubility and stability of the drug in aqueous media. Therefore, the drug must be soluble in appropriate solvents and it is very important that it does not precipitate in the aqueous environment (or at physiological conditions) and that it is stable (not degradable) in the timescale of the biochemical studies [**34-36**].

Upon entering the cell, the drug needs to reach the target or interact / interfere with the relevant cellular processes. Radical and reactive oxygen species (ROS) are related with many diseases such as inflammation, hypertension, coronary heart disease, atherosclerosis, Alzheimer's disease, Parkinson's disease etc. [**37**]. These free radicals are produced under certain environmental conditions and during normal cellular functions in the body. So, antioxidants play an important role to protect the human body against damage by radicals [**38**]. Consequently, evaluation of antioxidant activity of new compounds is desirable.

Many biological targets including, membranes, proteins and DNA have been used for evaluation of biological activities of compounds [**39**]. The anticancer activity of cisplatin is believed to result from its interaction with DNA. The drug reacts with nucleophilic sites in DNA forming monoadducts, as well as intra and inter strand crosslinks. This has been used as rationale to choose DNA as biological target to evaluate the anticancer activity of other metal complexes [**40**]. DNA regulates many biochemical processes that occur in the cellular system. The different loci present in the DNA are involved in various regulatory processes such as gene expression, gene transcription, mutagenesis, carcinogenesis, etc. Transition metal complexes can bind to DNA by both covalent and non-covalent interactions. Covalent binding involves the coordination of the nitrogenous base or the phosphate moiety of the DNA to the central metal ion. The non-covalent binding modes are intercalation, which involves the stacking of the molecule between the base pairs of DNA, groove binding, which comprises the insertion

of the molecule into the major or minor grooves of DNA and electrostatic or external surface binding [**5, 41**]. Among these, covalent binding and intercalation are among the most important DNA binding modes for therapeutic drugs. The DNA binding mode and strength of the affinity are affected by several factors, such as planarity of ligands, the coordination geometry, the ligand donor atom type, the metal ion type and its flexible valence [**5, 41, 42**].

1.8 Objectives

The main objective of the current work is to develop drugs to fight cancer and microbial diseases. Herein, we report the synthesis, characterization and solution behavior of zinc complexes with two ligands: an S-methyl dithiocarbazate Schiff base and 4-methyl-2,6-bis(pyridin-2-yl-hydrazonomethyl)-phenol. Stability in aqueous media and evaluation of antioxidant activity of the synthesised compounds are reported. The BSA and DNA binding ability of the zinc(II) complexes are also evaluated and discussed. The biological screening focused on their cytotoxic, antibacterial and antifungal activity.

2. Experimental

2.1 Materials and reagents

2,6-Diformyl-4-methylphenol, 2-hydrazino pyridine (from Sigma-Aldrich), S-methyl carbazate and $Zn(CH_3COO)_2.2H_2O$ (from Panreac) were used as supplied. Solvents such as ethanol, methanol (from Carlo Erba), DMSO (from Fisher Scientific), D_2O, DMSO-d_6 (from Euriso-top) were used. Phosphate buffered saline (PBS) was purchased from Sigma-Aldrich as tablets readily soluble in water (deionized water) giving 0.01 M in phosphate (NaCl, 0.138 M; KCl, 0.0027 M), pH 7.4 at 25 ºC. Defatted BSA (Sigma-Aldrich reference A-7511; ≥ 97 %) with molecular weight of 66,430 Da and *calf thymu*s DNA (*ct*DNA) were purchased from Sigma-Aldrich. Millipore® water was used in the experiments with biological molecules. All other materials not mentioned here were either analytical or reagent grade.

2.2 Instrumentation

Elemental analysis for C, H, N and S were carried on a FISONS EA 1108 CHNS-O apparatus at Laboratório de Análises of Instituto Superior Técnico. The NMR spectra were recorded at ambient temperature on a Bruker Avance II + 300 (Ultra Shield TM Magnet) spectrometer operating at 300.13 MHz. The ^{1}H NMR chemical shifts are reported in ppm using TMS (tetramethylsilane) as internal reference or the solvents' residual peak. The Infra-Red (FT-IR) spectra were recorded on Alpha RTDLaTGS HR 0.8 FTIR spectrophotometer and the UV-Visible absorption spectra were recorded on a Perkin Elmer Lambda 35 UV-Vis spectrophotometer with 10.0 mm optical path cuvettes. A 500-MS Varian Ion Trap Mass Spectrometer was used to measure ESI-MS spectra of methanolic solutions of the ligands and complexes in both positive and negative modes. Circular dichroism spectra were recorded on a JASCO J-720 spectropolarimeter (JASCO, Hiroshima, Japan) with UV-Vis (500 – 200 nm) photomultiplier (EXEL-308) at room temperature with a 10 mm quartz cell. The spectra were acquired at scanning speed of 200 nm/min; band-width of 2.0 nm; response of 2.0 sec; sensitivity of 100 mdeg and data pitch of 2 nm. Three accumulations were made for each measurement and the average was taken. Fluorescence measurements were carried out on a SPEX® Fluorolog spectrofluorimeter (Horiba Jobin Yvon) in a FL3-11 configuration, equipped with a Xenon lamp and in a 10 mm quartz cuvette. The instrumental response was corrected by means of a correction function provided by the manufacturer. The experiments were carried out at room temperature and all are steady-state measurements.

2.3 Synthesis of the ligands

4-methyl-2,6-bis(pyridin-2-yl-hydrazonomethyl)-phenol – L1 - A methanolic solution (43 mL) of 2-hydrazino pyridine (0.4651 g, 4.26 mmol) was added dropwise to a methanolic solution (32 mL) of 2,6-diformyl-4-methylphenol (0.3501 g, 2.13 mmol) with constant stirring for 30 min at room temperature. The mixture was refluxed for 5 h, cooled to room temperature and filtered. The yellow microcrystalline solid was collected, washed thoroughly with cold methanol and dried in vacuum. Yield: 74% (0.5436 g). ESI-MS (MeOH) *m/z* [calculated (Found)]: 347.16 (347.11) (100%) $[L1+H]^+$. Elemental analysis; $C_{19}H_{18}N_6O.0.5\ H_2O$; C, 64.21%; H, 5.39%; N, 23.65%. Found: C, 64.54%; H, 5.10%; N, 23.53%. FT-IR (KBr, cm^{-1}): 3411 (OH), 3194 (NH), 1599 (C=N). ^{1}H NMR (300 MHz, DMSO-d_6, δ(ppm)): 2.31 (s, 3H, C_7-H), 6.80 (t, 2H, C_{14} & $_{24}$ -H), 7.07 (d, 2H, C_{12} & $_{26}$ -H), 7.42 (s, 2H, C_3 & $_5$ -H), 7.68 (t, 2H, C_{13} & $_{25}$ -H), 8.17 (d, 2H, C_{15} & $_{23}$ -H), 8.33 (s, 2H, C_{14} & $_{24}$ -H), 11.05 (s, 2H, N-H), 11.71 (s, 1H, O-H). ^{13}C NMR (300MHz, DMSO-d_6, δ(ppm)): 20.10 (C_7), 121.14 (C_2 & $_6$), 128.34 (C_4), 138.47 (C_{15} & $_{23}$), 148.00 (C_8 & $_{18}$), 152.87 (C_1), 156.72 (C_{11} & C_{21}). UV-Vis [DMSO, λ_{max}/nm ($\varepsilon/M^{-1}cm^{-1}$)]: 369 ($7.17x10^4$), 345 ($1.53x10^5$), 331 ($1.47x10^5$).

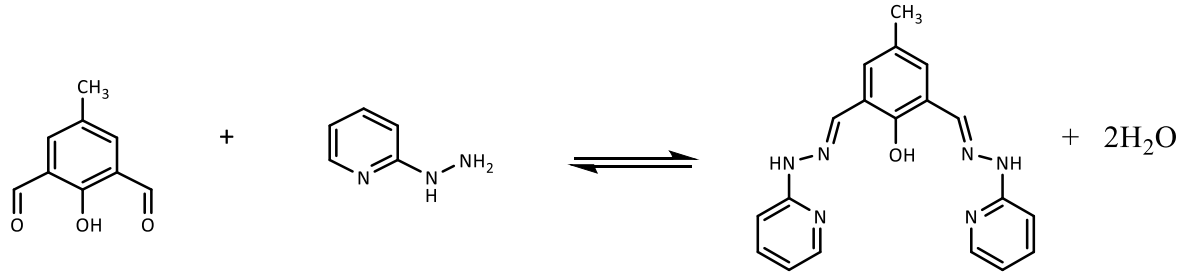

Scheme 3 Synthesis of **L1**.

Methyl-phenol-di-S-methyl dithiocarbazate - L2 - A methanolic solution (4 mL) of S-methyl carbazate (0.3918 g, 4.34 mmol) was mixed with a methanolic solution (12 mL) of 2,6-diformyl-4-methyl phenol (295.7 mg, 1.80 mmol) with stirring. The mixture became cloudy and a yellow solid formed. It was refluxed for 4 h, cooled to room temperature and a yellow solid was filtered, washed with methanol followed by petroleum ether and dried in vacuum. Yield: 78% (0.5251 g). ESI-MS (MeOH) *m/z* [calculated (Found)]: 371.55 (371.03) (100%) $[L2-H]^-$. Elemental analysis; $C_{13}H_{16}N_4OS_4.1.5H_2O$, C, 39.08%; H, 4.79%; N, 14.02%, S, 32.10. Found: C, 39.32%; H, 4.06%; N, 13.70%, S, 32.24. FT-IR (KBr, cm^{-1}): 3119 (OH), 2982 (NH), 1617 (C=N), 1518 (C=C), 1320 (C-O), 1044 (C=S), 770 (C-S). ^{1}H NMR (300MHz, DMSO-d_6, δ(ppm)): 2.33 (s, 3H, C_7-H), 2.59 (s, 6H, C_{14} & C_{22} -H), 7.57 (s, 2H, C_3 & C_5 -H),

8.53 (s, 2H, C_8 & C_6 -H), 10.81 (s, 1H, O-H), 13.52 (s, 2H, N-H). ^{13}C NMR (300MHz, DMSO-d_6, δ(ppm)): 16.81 ($C_{14\ \&\ 18}$), 19.79 (C_7), 119.65 ($C_{2\ \&\ 6}$), 129.61 (C_4), 131.31 (C_{3} & $_{5}$), 144.75 ($C_{8\ \&\ 16}$), 154.54 (C_1), 197.45 ($C_{11\ \&\ 19}$). UV-Vis [DMSO, λ_{max}/nm (ε/$M^{-1}cm^{-1}$)]: 371 (1.07x10^5), 345 (1.53x10^5), 332 (1.46x10^5).

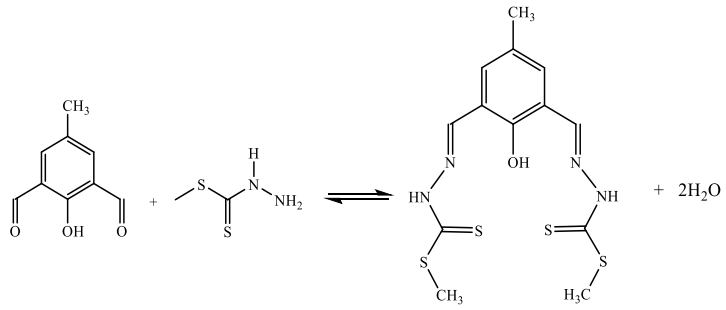

Scheme 4 Synthesis of **L2**.

2.4 Synthesis of complexes

$[Zn_2(L1)(OAc)_3]$ (C1) - An ethanolic solution (3 mL) of $Zn(CH_3COO)_2.2H_2O$ (228.7 mg, 1.04 mmol) was added dropwise to a solution of **L1** (181.1 mg, 0.523 mmol) in ethanol (32 mL) with constant stirring for 30 min at room temperature. The mixture was refluxed for 2 h, and then cooled to room temperature. Finally, an orange coloured compound was separated from the reaction mixture, washed thoroughly with petroleum ether and dried in vacuum. Yield: 50% (0.1693 g). ESI-MS (MeOH) *m/z* [calculated (Found)]: 409.08 (409.31) (100%) $Zn(L1)^+$, 266.0 (266.12) (20%) $Zn_2(L1)(OAc)^{2+}$. Elemental Analysis for $C_{25}H_{26}N_6O_7Zn_2.H_2O$; C, 44.57%; H, 4.23%; N, 12.47%. Found: C, 44.42%; H, 4.17%; N, 12.97%. FT-IR (KBr, cm^{-1}): 3012 (NH), 1629 (C=N), 1560 (C=C), 772 (C-H), 673 (Zn-O), 479 (Zn-N). ^{1}H NMR (300 MHz, DMSO-d_6, δ(ppm)) 2.23 (s, 3H, C_7-H), 6.54 (t, 2H, C_{14} & $_{24}$ -H), 6.62 (d, 2H, C_{12} & $_{26}$ -H), 7.10 (s, 2H, C_3 & $_5$ -H), 7.51 (t, 2H, C_{13} & $_{25}$ -H), 7.80 (d, 2H, C_{15} & $_{23}$ -H), 8.20 (s, 2H, C_{14} & $_{24}$ -H)

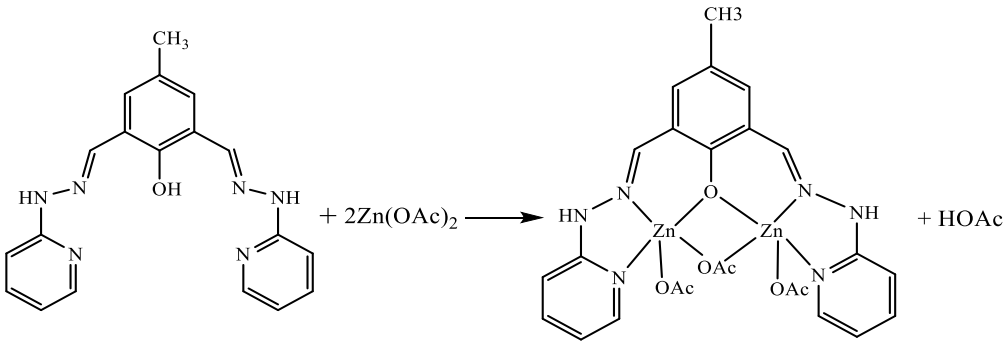

Scheme 5 Synthesis of **C1**.

[Zn_2(L2)(OAc)] (C2) - Complex **C2** was synthesized in a similar procedure as the one used for **C1**, with **L2** (166 mg, 0.446 mmol) instead of **L1,** where a yellow coloured compound separated out from the reaction mixture which was filtered, washed thoroughly with petroleum ether and dried in vacuum. Yield: 57% (0.1732 g). ESI-MS (MeOH) m/z [calculated (Found)]: 198.15 (98.58) (40%) ($Zn(L2)H_3^{3+}$, 496.86 (497.09) (2%) $Zn_2(L2)^+$, 434.94 (434.29) (10%) $Zn(L2)H^+$. Elemental Analysis for $C_{16}H_{20}N_4O_4S_4Zn_2$; C, 32.50%; H, 3.41%; N, 9.47%, S. 21.68 Found: C, 32.48%; H, 3.14%; N, 9.75%, S, 21.31. FT-IR (KBr, cm^{-1}): 2920 (NH), 1618 (C=N), 1548 (C=C), 1317 (C-O), 965 (C-S), 772 (C-H), 673 (Zn-O). ^{1}H NMR (300 MHz, DMSO-d_6, δ(ppm)) 2.23 (s, 3H, C_7-H), 6.54 (t, 2H, $C_{14\,\&\,24}$ -H), 6.62 (d, 2H, $C_{12\,\&\,26}$ -H), 7.10 (s, 2H, $C_{3\,\&\,5}$ -H), 7.51 (t, 2H, $C_{13\,\&\,25}$ -H), 7.80 (d, 2H, $C_{15\,\&\,23}$ -H), 8.20 (s, 2H, $C_{14\,\&\,24}$ -H)

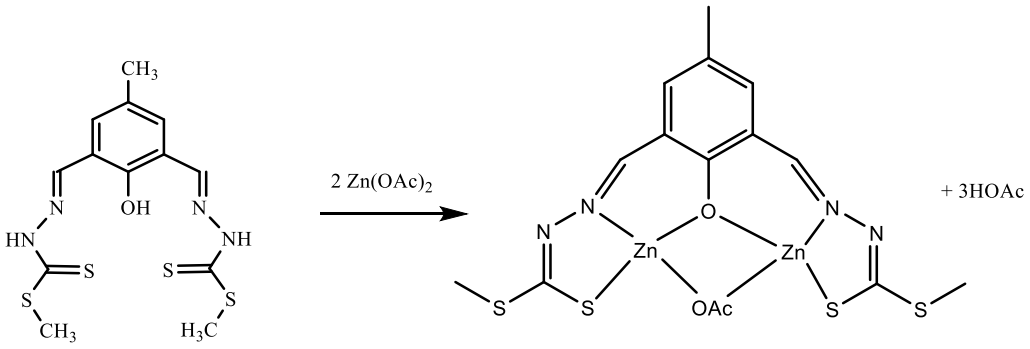

Scheme 6 Synthesis of **C2**.

2.5 Stability studies in aqueous medium

The stability of the Zn(II) complexes was evaluated using UV-Vis and NMR spectroscopies. UV-Vis absorption experiments were done using final concentrations of 25 μM (DMSO, 3% v/v) in PBS buffer (10 mM, pH 7.4) in the absence and presence of bovine serum albumin (BSA, 25 μM). The UV-Visible spectra (250-600 nm) were recorded for six consecutive hours and the spectra were measured again after 24 hours. Stability of complex **C1** (25 μM, 2% DMSO v/v) was also followed in cell culture medium with and without FBS (10 % v/v). The UV-Visible spectra (250-600 nm) of the complex were recorded for six hours and measured again after 24 hours. The stability study of complex **C1** was also carried out by ^{1}H NMR. 12.5 mg of **C1** were dissolved in 250 μl of DMSO-d_6. Then, 20 μl of this solution were mixed with 380 μl of the phosphate buffer giving 5 % DMSO and 95 % D_2O. Finally, the stability of the compound was studied for 24 h by ^{1}H-NMR spectroscopy.

2.6 BSA binding studies

Stock solutions of BSA were prepared in buffer solution (PBS, 10 mM, pH 7.4 at 25°C) and kept overnight to hydrate. The concentration of BSA stock solutions ranged from *ca.* 34 to 918 μM, which was estimated considering the molar extinction coefficient (279 nm, 44,309 M^{-1} cm^{-1}) [**43**]. The concentration of stock solutions of Schiff base ligands and complexes was between *ca.* 100 to 5370 μM which were prepared by dissolving the compounds in spectroscopic DMSO.

2.6.1 UV–visible spectroscopic titrations

Electronic absorption titrations were performed by successive additions of BSA stock solutions, *ca.* 750 - 900 μM, to solutions of compounds in 4% (v/v) of DMSO-PBS (10 mM, pH 7.4) where a similar volume of BSA was also added to the reference cell. The initial concentration of compounds was set at *ca*. 25-29 μM and the molar ratio of BSA to compound varied between 0 and 4. The absorption spectra were recorded from 270 to 700 nm at room temperature. All the experiments were performed in phosphate buffer saline (10 mM, pH 7.4) in a conventional quartz cell (10.0 mm).

2.6.2 Circular dichroism spectra

To evaluate the structural changes of BSA induced by the addition of compounds, circular dichroism (CD) spectra were measured in solution. The technique is appropriate because BSA has a high percentage of α-helical structure, which shows a characteristic CD signal in the Far-UV region. Predominately α-helical proteins show two strong negative bands with maxima at 209 and 220 nm. Changes in the intensity of these bands reflect changes in the amount of helicity of BSA [**44**]. Stock solutions of protein (34.12 - 100 μM) were prepared in buffered solutions (PBS, 10 mM, pH 7.4). Spectral changes of BSA were monitored after adding different concentrations of compounds (0 –3 μM) to the BSA solution.

2.6.3 Spectrofluorimetric titrations

Working solution of BSA was obtained by diluting stock solution to a concentration of 1.16 μM (for **L1**, **L2** and **C1** assays) and 1.25 μM (for **C2** assay) in PBS buffer with final volume of 2520 μl in 10 mm path length quartz cuvette. The intrinsic fluorescence emission quenching experiments of BSA were done by successive additions of the compounds to obtain final concentrations ranging from 0.20 - 5.81 μM with DMSO < 5% *v/v*, where individual working

solutions were prepared to obtain molar ratios of BSA: Compounds ranging from 1:0 to 1:6. All spectra were recorded by allowing solutions to equilibrate after every addition of the compounds. The fluorescence emission spectra were recorded between 295 and 400 nm by exciting at 285 nm (λ_{ex} = 285 nm) with slits of 3 nm. UV-visible absorption spectra were recorded for each sample to correct the absorption and inner filter effects of the fluorescence emission intensities. All spectra were collected in the S/R mode and corrected for optics and detector wavelength dependence. Moreover, blank assays were done for each system where the fluorescence spectra for solutions containing the same concentration of compound without BSA were recorded and subtracted from the corresponding emission spectra containing the fluorophore.

Successive additions of the compounds under the same conditions cause fluorescence quenching, a decrease in the emission fluorescence intensity of BSA at emission max (λ_{max} = 340 nm), and the fluorescence quenching can be analysed by the Stern-Volmer equation (**Equation 1**) [**45**].

$$F_0/F = 1+K_{sv}[Q] = 1+K_q\tau_0[Q] \qquad (\mathbf{1})$$

where F and F_0 are BSA fluorescence intensities in the presence and absence of quencher (metal complexes), respectively. K_q, K_{sv}, τ_0 and [Q] are the quenching rate constant, the Stern-Volmer quenching constant, the average biomolecule lifetime in the absence of quencher and the quencher concentration, respectively.

2.7 DNA interaction studies

All the experiments involving the interaction of ligands and complexes with *ct*DNA were carried out in buffered solution (PBS, 10 mM, pH 7.4) at room temperature. Stock solutions of DNA were prepared by dissolving the nucleic acid in buffered solution (PBS, 10 mM, pH 7.4 at 25°C), keeping it at 4ºC for about 2 days to allow dissolution of the DNA and used within a week. The concentration of the prepared *ct*DNA stock solutions were calculated based on their absorbance at 260 nm by using their per nucleotide extinction coefficient ε_{260} = 6600 M^{-1} cm^{-1} [**46**]. Solutions of DNA gave ratios of absorbance A_{260}/A_{280} of *ca.* 1.9, indicating that the DNA was sufficiently pure and free of protein [46].

2.7.1 UV-Vis spectroscopy

Stock solutions of both ligands and complexes were prepared in DMSO with concentration of 2.65 and 1.54 mM for ligands **L1** and **L2,** respectively; and 1.53 mM for **C1** and **C2**. Then further dilutions were made in PBS buffer (pH 7.4 10 mM) having final concentrations of *ca.* 37.8 μM for **L1** and *ca.* 25 μM for **L2** and complexes. Absorption titration experiments were performed by maintaining the compounds' concentration roughly constant and increasing the concentration of DNA to obtain ratios of [compound]/[DNA] ranging from 1:0 to 1:2.4 for **L1** and from 1:0 to 1:4 for the rest of the compounds. To eliminate the contribution of the absorbance of *ct*DNA itself, an equal quantity of *ct*DNA was added to both the sample and the reference solutions. All solutions were incubated for 4 - 5 min before absorption spectra were recorded. The titration kept going until there were no changes in the spectra, indicating that binding saturation was achieved.

2.7.3 Circular dichroism spectra

Circular dichroism (CD) is a useful technique for monitoring DNA conformational changes resulting from changes in environmental conditions, such as temperature, ionic strength, and pH, and for the study of the interaction between DNA and compounds. Circular dichroism studies were done in quartz SUPERASIL© cuvettes of 10 mm optical path. The *ct*DNA solution was prepared by dilution of the stock solution (2.56 mM) in PBS buffer (pH 7.4, 10 mM) to obtain a final concentration of *ca.* 60 μM in each sample. Stock solutions of ligands and Zn-complexes, *ca.* 5.7 mM in DMSO were prepared. Spectra were recorded by keeping the concentration of DNA constant while varying the concentration of ligands and complexes from 0 to 260 μM to obtain DNA: compound ratios ranging from 1:0 to 1:4.5. After every addition, the samples were allowed to equilibrate for a few minutes before spectral measurements. PBS buffer solution was used to obtain the baseline, which was subtracted from each CD spectrum. The spectra were collected from 200 - 500 nm with a resolution of 1.0 nm, with band-width of 1.0 nm, scan speed of 200 nm/min, 2.0 s response time and 3 accumulations were taken and averaged. The recorded spectra (in millidegrees) were converted into Δε expressed in $M^{-1}cm^{-1}$ using the concentration of *ct*DNA and the cell path length (1 cm). The processing of the CD spectra was done using JASCO32 software.

3. Results and Discussion

In this work zinc complexes of Schiff bases 4-methyl-2,6-bis(pyridin-2-yl-hydrazonomethyl)-phenol (**L1**) and methyl-phenol-di-S-methyl dithiocarbazate (**L2**) were prepared and studied. The Schiff base ligands were synthesized by condensation of an aromatic dialdehyde with 2-hydrazino pyridine and S-methyl dithiocarbazate in methanol at refluxing temperature for 4-5 h to yield **L1** and **L2**, respectively. Complexes were prepared from the reaction of zinc acetate with the Schiff bases in methanol/ethanol at room temperature for 15-30 min and then at refluxing temperature for 2 h. Percentage yields of the reactions ranged from 74 – 78% for the Schiff bases and 49 – 56% for the zinc complexes. All synthesized compounds were soluble in DMSO.

Upon complexation of the metal ion with S-substituted dithiocarbazate derived Schiff base ligand, deprotonation of the nitrogen of the dithiocarbazate is expected, leading to an iminothiolate and coordination via NS atoms is anticipated.

3.1 Characterization

To confirm the formation of the metal complexes and to characterize them, several techniques were employed. The proposed structures and stoichiometries were initially established by elemental analysis and mass spectrometry. The analytical data for ligands and metal complexes agreed well with the formulations proposed. All the mass spectra show signals corresponding to the molecular weight of either the protonated complexes or adducts formed with solvent molecules. Elemental analysis and various spectroscopic characterization results are discussed in the following sections.

NMR spectroscopy is very important to determine the groups through which the ligands form their corresponding metal complexes and confirm the proposed structures. ^{1}H and ^{13}C NMR experiments were done for all ligands and zinc complexes. ^{1}H NMR spectra were recorded at room temperature using DMSO-d_6 as solvent and the chemical shifts are given in **Tables 1** and **3,** whereas ^{13}C NMR data is given in **Tables 2** and **4**. ^{1}H NMR spectroscopy allowed the identification and attribution of the peaks making a perfect correspondence both in the chemical shift and integration values to the proposed structures depicted in **Figure 6**. An important peak assignment is the one corresponding to the azomethine protons (**H**C=N), which clearly confirms the formation of the Schiff bases [**49 - 52**].

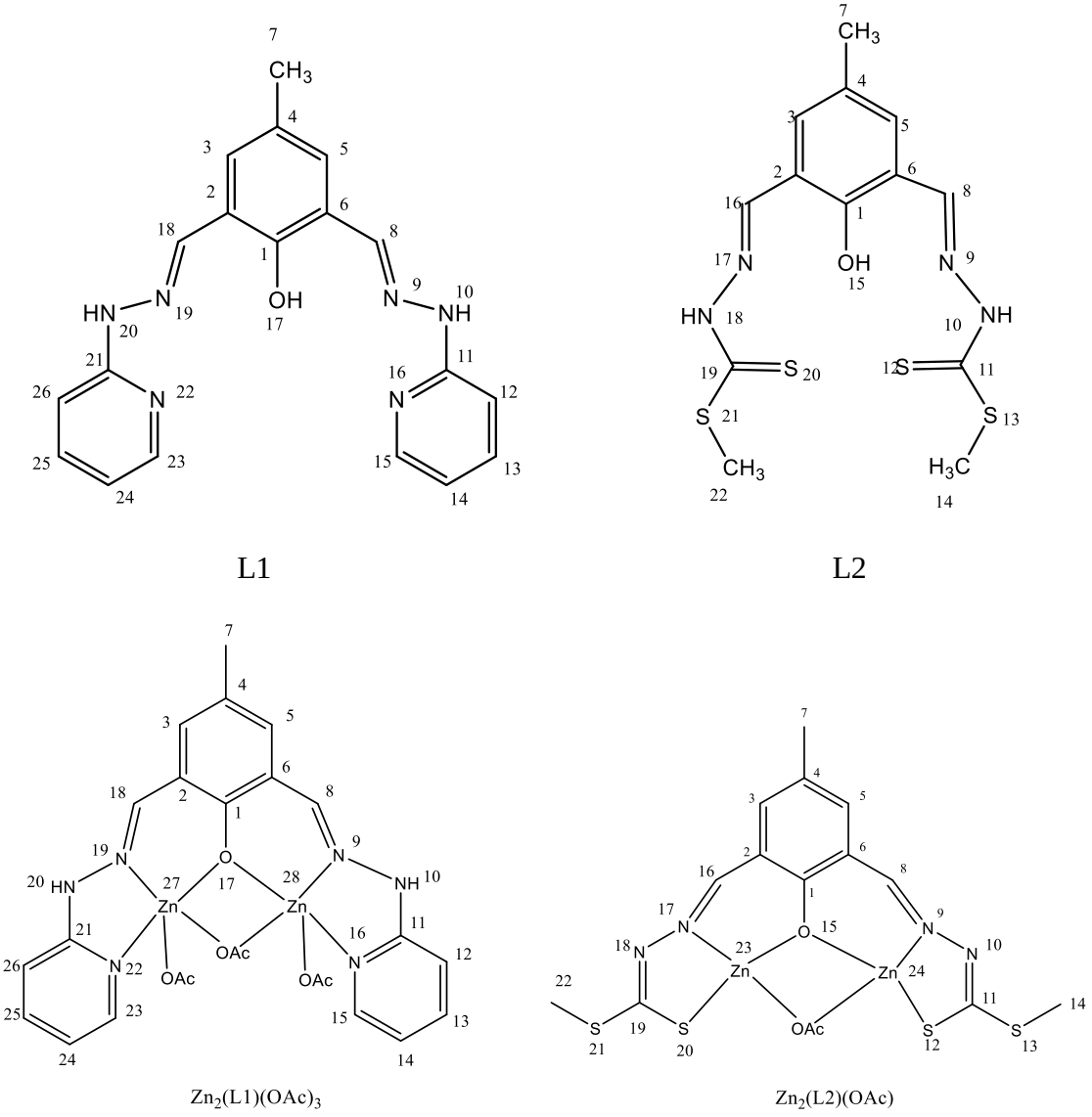

Figure 6 Structure of Schiff base ligands and complexes synthesised with the atom labelling scheme used in the NMR characterization.

The ^{1}H NMR spectra of the Schiff base ligands show a broad peak ranging from 10.81-11.71 ppm attributed to phenolic hydroxyl protons [**48 - 50**]. The absence of this peak in the spectra of complexes **C1** and **C2** confirms the involvement of deprotonated hydroxyls in chelation to the metal ion [**50, 51**]. The peaks displayed by ^{1}H NMR spectra of Schiff bases in the range δ = 8.33–8.53 ppm were attributed to the azomethine protons (**H**C=N) [**48 - 51**]. The spectra of the complexes exhibited the azomethine proton signals shifted downfield which confirms the formation of the metal complex, with binding through these donors [**50, 51**].

Signals of aromatic protons were observed in the chemical shift range 6.80–8.17 ppm and aliphatic protons showed up at 2.31 ppm [**52**]. The signals of ^{13}C NMR assigned to the chemical shift of methyl groups for the two ligands were observed at 16.81 and 20.10 ppm [**53**], while the signals of aromatic carbons were in the range of 119.65–156.72 [**53, 54**]. The signals observed at 145.75 and 148.00 ppm, were attributed to the chemical shifts of azomethine carbons, which confirm the formation of the Schiff bases [**55, 56**].

Table 1 ^{1}H NMR chemical shifts (δ /ppm) and assignment for **L1** and **C1** in DMSO-d_6.

Compound	δ/(multiplicity, number of protons)						
	$H_{14\ \&24}$	$H_{12\ \&\ 26}$	$H_{3\ \&\ 5}$	$H_{13\ \&\ 25}$	$H_{15\ \&\ 23}$	HC=N	Ar-OH
L1	6.8 (t, 2H)	7.1 (d, 2H)	7.4 (s, 2H)	7.7 (t, 2H)	8.2 (d, 2H)	8.33 (s, 2H)	11.05 (s, 1H)
C1	6.5 (t, 2H)	6.6 (d, 2H)	7.1 (s, 2H)	7.5 (t, 2H)	7.8 (d, 2H)	8.21 (s, 2H)	-

Table 2: ^{13}C NMR chemical shifts (δ/ppm) and assignment for **L1** and **C1** in DMSO-d_6.

Compound	δ/(ppm of ^{13}C)				
	C_2 & C_6	C_4	C_{15} & C_{23}	C_8 & C_{18}	C_{11} & C_{21}
L1	121.14	128.34	138.47	148.00	156.72
C1	125.03	125.03	145.37	156.76	162.13

Table 3 ^{1}H NMR chemical shifts (δ /ppm) and assignments for **L2** and **C2** in DMSO-d_6.

Compound	**δ/(multiplicity, number of protons)**				
	$H_{14\ \&\ 22}$	**$H_{3\ \&\ 5}$**	**-NH**	**Ar-OH**	**HC=N**
L2	2.59 (s, 6H)	7.57 (s, 2H)	13.52 (s, 2H)	10.81 (s, 1H)	8.33 (s, 2H)
C2	3.28 (s, 6H)	7.41 (s, 2H)	-	-	8.68 (s, 2H)

Table 4 ^{13}C NMR chemical shifts (δ /ppm) and assignment for **L2** and **C2** in DMSO-d_6.

Compound	δ/(ppm of ^{13}C)			
	C_{14} & C_{22}	C_2 &C_6	C_3 & C_5	C_8 & C_{16}
L2	16.8	119.7	131.3	144.8
C2	14.7	120.7	139.8	160.4

The aromatic protons and carbons of ligands in the ^1H and ^{13}C NMR spectra appear around 6.8-8.2 ppm and 119.7-156.7 ppm, respectively, which were shifted to 6.5- 7.8 ppm and 120.0-162.13 ppm, respectively, in the Zn(II) complexes.

a)

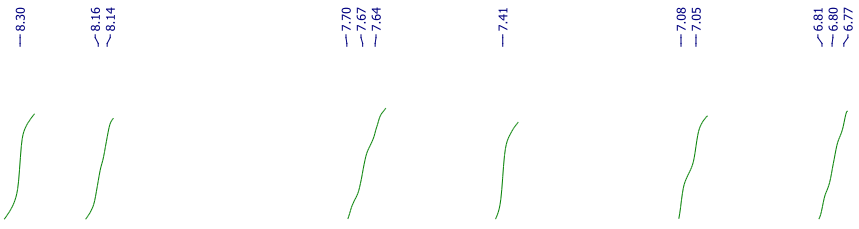

L1

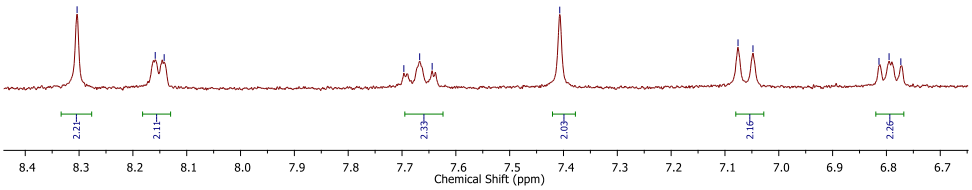

b)

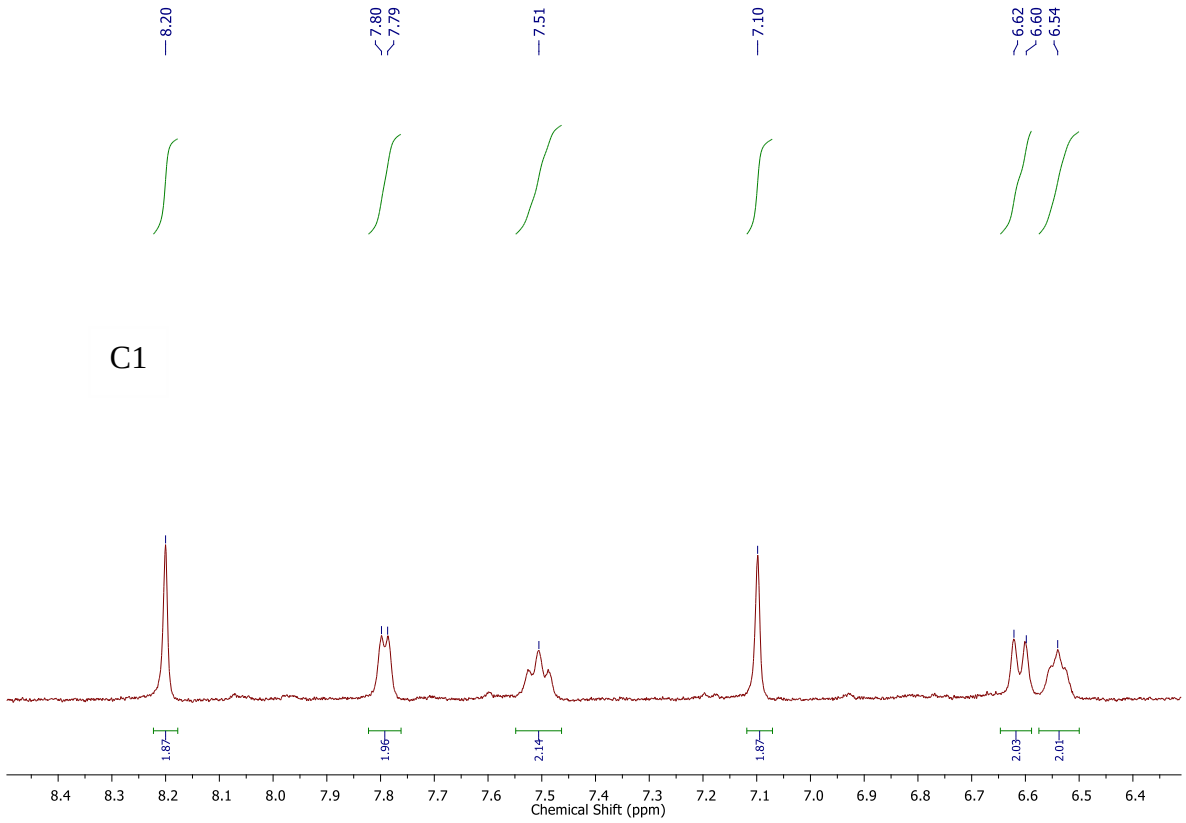

Figure 7 Aromatic region of the ^{1}H NMR spectra of (a) **L1** and (b) **C1** in DMSO-d_6 at room temperature.

The electronic absorption spectra of the ligands and their metal complexes in DMSO were scanned in the region 270 – 700 nm at concentrations of 25 μM and the results are depicted in **Fig. 8**. In the spectra of the Schiff base ligands it was possible to observe two set of bands corresponding to the π → π* and n → π* transitions of imine bonds present in the molecules [**56**]. The ligands exhibited high intensity bands which appeared at wavelengths of *ca.* 330 and 380 nm which were assigned to π→π* and n→π* transitions, respectively. For metal complexes, the first band at *ca.* 310 - 370 nm corresponding to the π→π* transition was observed, whereas the second intra-ligand band at higher wavelength *ca*. 430 - 480 nm ascribed to n→π* band showed either a blue shift with a reduction of intensity or disappeared. This is due to donation of the lone pair of electrons to the metal and hence the coordination of the azomethine group [**57**]. Both of Zn(II) complexes showed the presence of ligand-to-metal charge transfer (LMCT) band (400 - 450 nm).

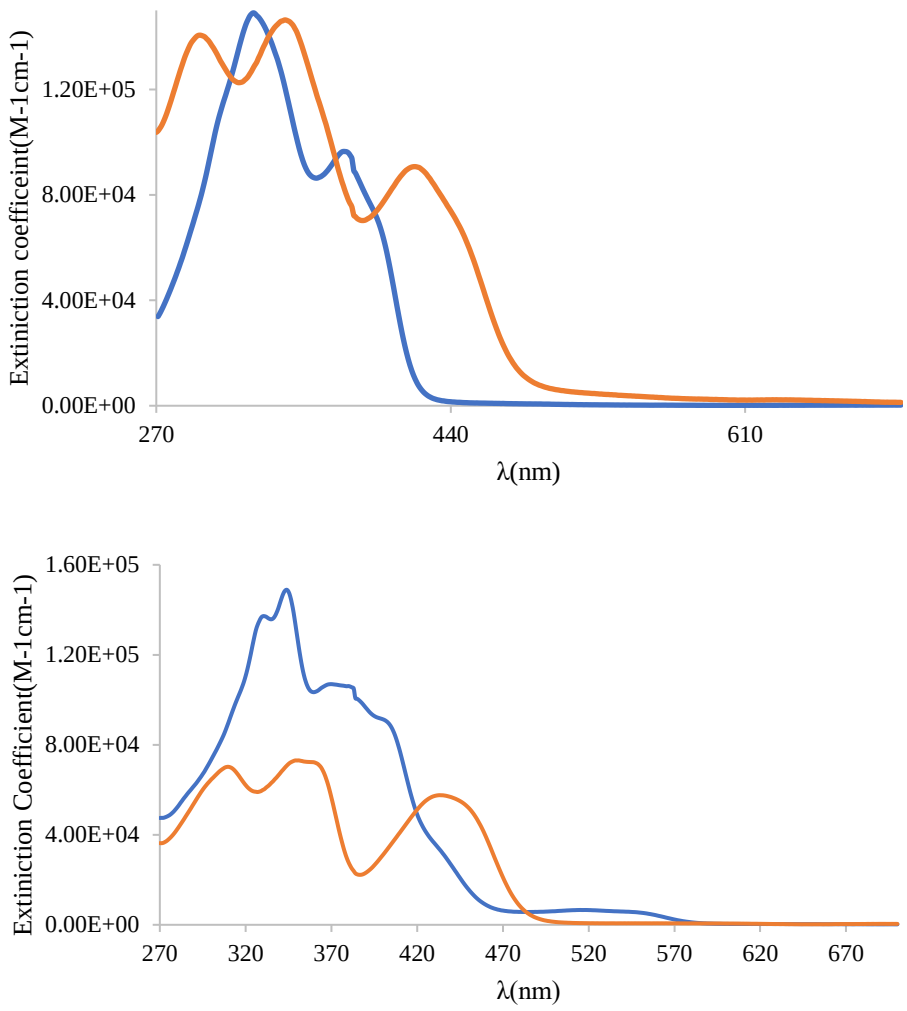

Figure 8 UV-Visible absorption spectra for Schiff base ligands and their corresponding Zinc complexes in DMSO at room temperature.

The ligands and complexes were also characterized by electrospray ionization mass spectrometry (ESI-MS) and it was possible to assign the peak corresponding to the molecular ion for both ligands, according to the expected molecular weight [**58**], as shown in **Table 5**. The complexes are very hard to ionize and only a few peaks were assigned.

Table 5 Assignment of ESI-MS peaks for Schiff base ligands and their corresponding zinc(II) complexes.

Species	m/z (%)	
	Theoretical	Found
$L1+H^+$	347.16	347.11(100%)
$L2-H^-$	371.55	371.03(100%)
$Zn(L2)H_3^{3+}$	198.15	98.58 (40%)
$Zn(L1)^+$	409.08	409.31(100%)
$Zn_2(L1)(OAc)^{2+}$	266.0	266.12 (20%)
$Zn_2(L2)^+$	496.86	497.09(2%)
$Zn(L2)H^+$	434.94	434.29(10%)

The nature and functional groups attached to metal atoms can be provided by FTIR spectra. The IR spectra of zinc complexes were compared with that of corresponding Schiff base ligands where changes that have taken place during complexation are a confirmation for formation of the complexes. The complexes exhibited IR bands approximately around 3447 cm^{-1} due to ν(OH), which refer to water molecules present in the complexes lattice. Upon complexation, the band of the azomethine group which in the ~~of~~ free ligands appeared at 1599 and 1617 cm^{-1} (in **L1** and **L2**, respectively) shifted to 1629 and 1654 cm^{-1} for **C1** and **C2** respectively, indicating the coordination of the azomethine nitrogen atom to the metal ion. Furthermore, the coordination is further confirmed by appearance of new bands around 680-684, 519 - 580 and 471 - 502 cm^{-1} due to ν(Zn-N), ν(Zn-O) and ν(Zn-S), respectively. Other bands like $\nu(C\text{-}H)_{Ar}$ and ν(C=C) appear around 3050 cm^{-1} and 1490 cm^{-1}, respectively [**59, 60**]. Characteristic infrared bands of the Schiff base ligands and their complexes are listed in **Table 6** together with their assignments.

Table 6 IR spectral assignments (cm^{-1}) of ligands and complexes.

Compound	ν/(cm^{-1})				
	OH	N-H	C=N	Zn-N	Zn-O
L1	3441	3194	1599	-	-
L2	3119	2982	1617	-	-
C1	-	3012	1629	673	670
C2	-	3177	1654	682	596

Elemental analysis data on the percentage of carbon, hydrogen and nitrogen in all ligands and complexes were fairly in agreement with calculated values for the proposed structures as shown in the **Table 7**. Both Zn-complexes contain two Zn ions per ligand molecule. In **C1** three molecules of acetate are present probably coordinated to the Zn atoms, and in **C2** only one. Solvation molecules of water and/or MeOH are also present in the isolated solids. These findings/formulations are corroborated by the NMR studies, which show equivalence between both halves of the molecules.

Table 7 Analytical data for Schiff base ligands and their corresponding Zn(II) complexes.

Compound	Elemental Analysis calculated (found) (%)			
	C	H	N	S
L1	64.21 (64.5)	5.39 (5.1)	23.7 (23.5)	-
L2	39.1 (39.3)	4.8 (4.10)	14.0 (13.7)	32.1 (32.2)
C1	45.34 (45.96)	4.11 (4.01)	12.69 (12.86)	-
C2	32.50 (32.37)	3.41 (3.14)	9.47 (9.77)	21.68 (21.31)

3.2 Stability studies in aqueous medium

Since biological studies are typically done in aqueous media at physiological pH, in order to proceed with studies with biological molecules, it is necessary to ensure that the complexes do not precipitate in the aqueous environment, and that they are stable in the timescale of the studies. Thus, the stability of the Schiff base ligands and complexes was evaluated with UV-vis spectroscopy in pH 7.4 buffered solutions containing a minimum amount of organic solvent, which is used to dissolve the compounds. Phosphate Buffer Saline (PBS) was chosen due to its composition, since the osmolarity and ion concentrations of the solution match closely those of the human body. Changes observed with time for each ligand and complex solution were followed with UV-vis spectroscopy using 5% of DMSO and 95% PBS. Except for a slight decrease in absorbance values due to precipitation, the ligands, **L1** and **L2** and corresponding complexes **C1** and **C2** spectra maintain their original form. It was observed that the stability in aqueous media increased upon formation of the complexes. Overall no significant changes were observed in the complexes' spectra as seen in **Fig. 9**.

Observed changes may be due to low solubility of the complexes in the aqueous media and therefore if lower concentrations are used in the assays with biological molecules both the stability and the solubility are not compromised. Therefore, it can be assumed that synthesised compounds are found to be stable in the physiological environment to undergo necessary reactions required for bioactivity.

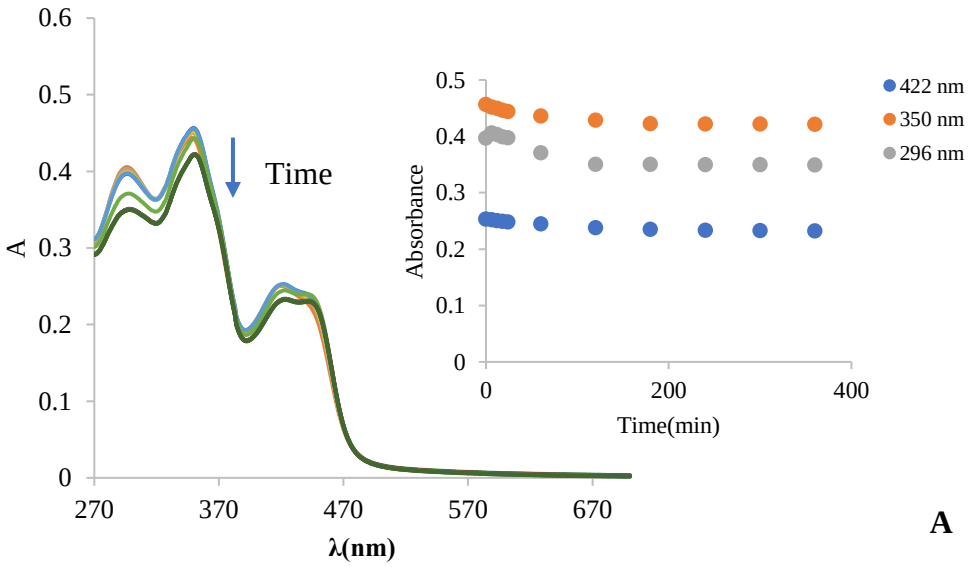

A

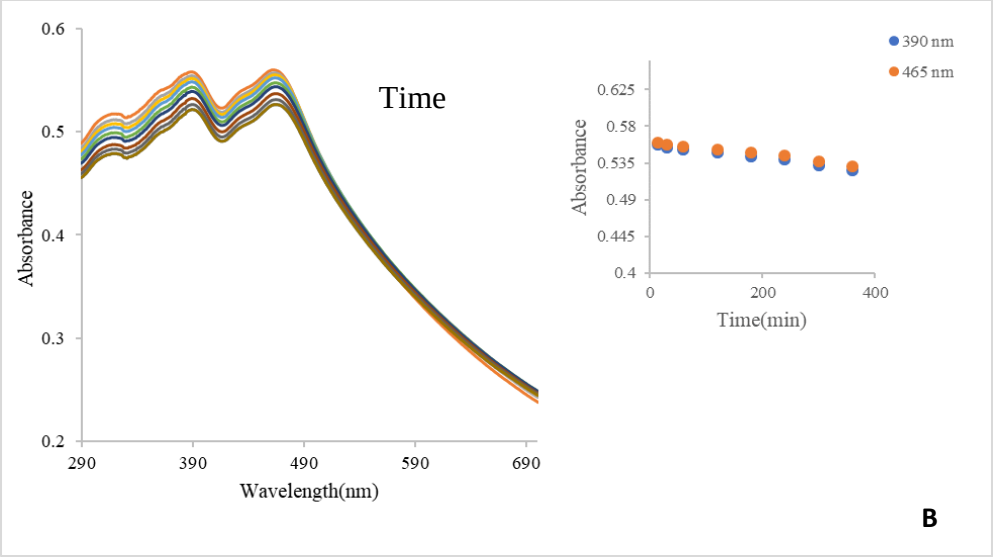

Figure 9 UV-Vis absorption spectra of **C1** (**A**) and **C2** (**B**) measured with increasing time (for 6 consecutive hours and again after 24h) for solutions containing 25 µM for each complex in PBS buffer with 3% DMSO. Inset: Variation at maxima (λ= 296 nm, 296 nm and 422 nm for **C1**, and λ= 390 nm and 465 nm for **C2**) in the first 400 minutes

Stability of complex **C1** (25 µM, 3%DMSO) was also followed in cell culture medium. The UV-Visible spectra (250-600 nm) of the complex, which were recorded for six consecutive hours and again after 24 hours (**Fig. 10)**, show that the complex is stable in this medium although there is a decrease in absorbance due to precipitation.

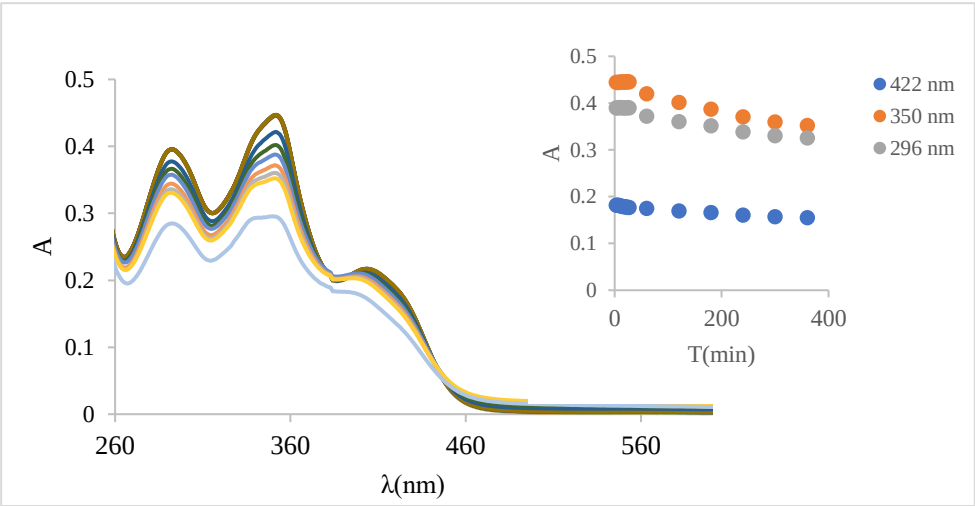

Figure 10 UV-Vis absorption spectra of C1 measured with increasing time (for 6 consecutive hours and again after 24h) for solutions containing 25 µM for the complex in cell culture medium with 3% DMSO. Inset: Variation at maxima (λ= 296 nm, 350 nm and 422 nm) in the first 400 minutes.

^{1}H NMR spectroscopy was also used to study the stability of **C1** in D_2O monitoring the ^{1}H NMR for 3 h and finally after 24 h. It was apparent from the measured spectra that the compound is stable in aqueous solution without hydrolysis except a simple shift of the peak at 8.25 to 7.7-7.8 due to the addition of D_2O. The proton integrations show that in the aromatic region there are still 6 protons making up a total of 12 protons as shown in the **Fig. 11**.

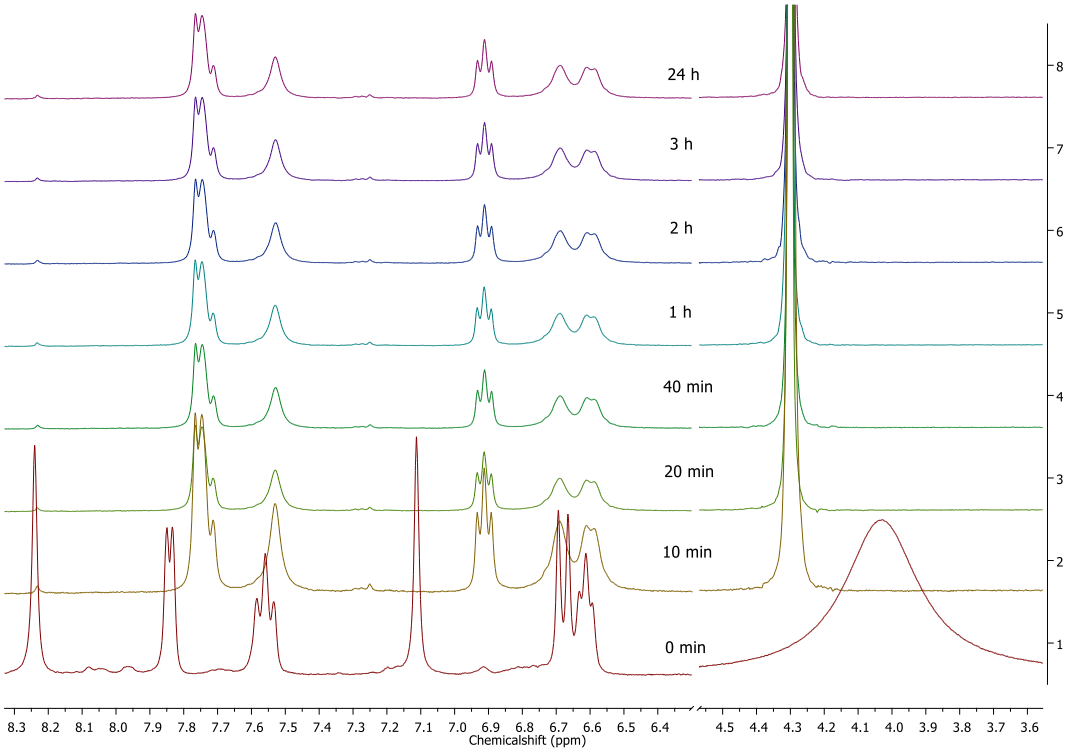

Figure 11 ^{1}H NMR spectra of **C1** in DMSO-d_6:D_2O, 5:95 %(*v/v)* measured with time.

3.3 Interaction with biomolecules

3.3.1 UV–visible BSA titrations

UV–visible absorption spectroscopy is a simple, useful technique to investigate conformational changes of proteins, even at low concentrations. This method is applicable to knowing the change in hydrophobicity [**60**] and the interaction between a drug and proteins [**61**]. **Fig. 12** show the electronic absorption spectra of the compounds in the absence and presence of increasing concentrations of BSA where the ratio of [BSA]/[compound] varied from 0.0 - 4.0 in buffered solution (PBS, 10 mM pH 7.4). The maximum absorption of the compounds exhibited a slight hypsochromic shift (hyperchromic for **C2**) in general by the incremental addition of BSA. These changes indicate that the compounds change its environment in the presence of BSA suggesting binding between the two.

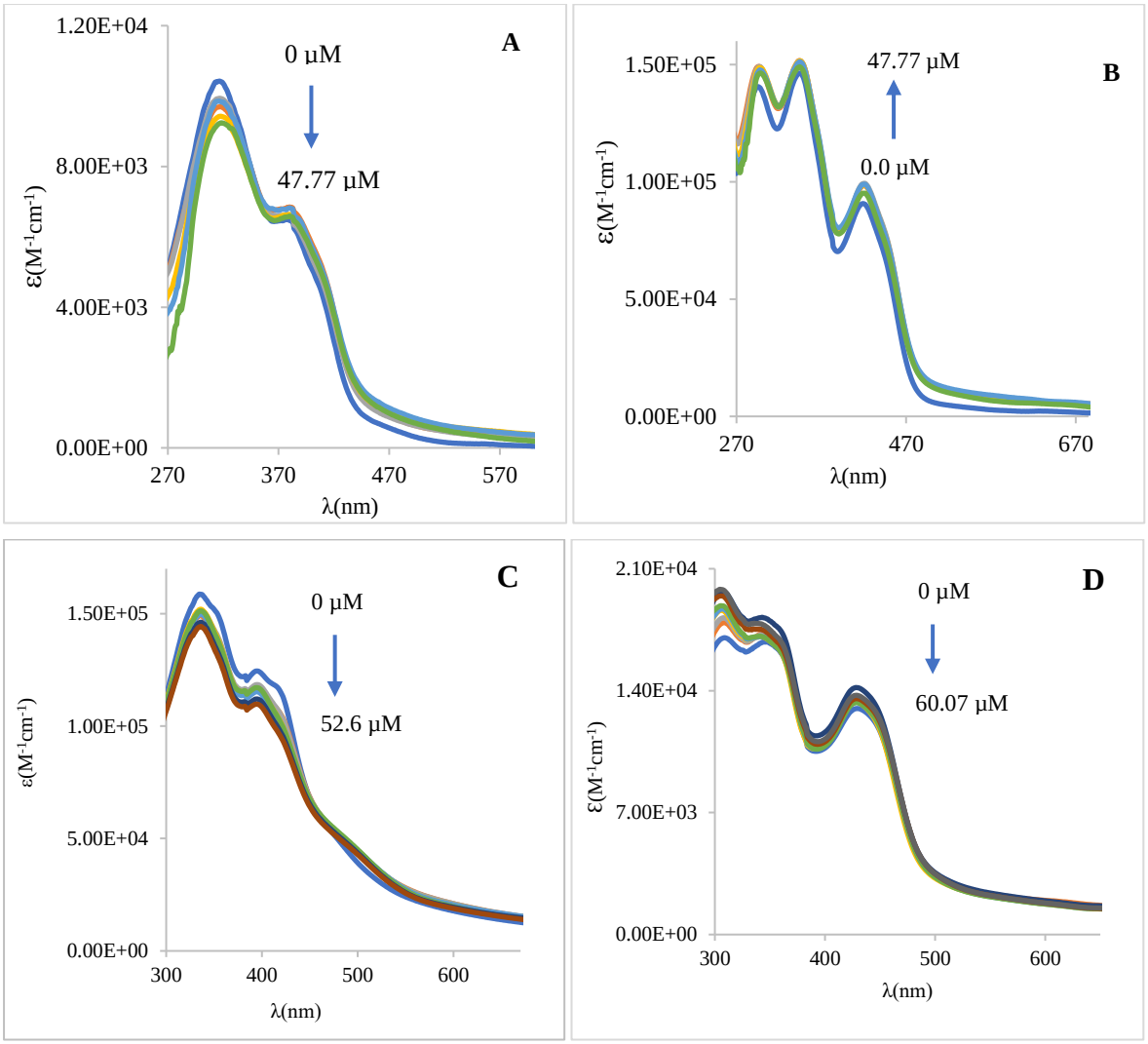

Figure 12 UV-visible absorption spectra of (A and B) 2.5 x 10^{-5} M **L1** and **C1** in the absence and presence of 0, 5.3, 12.6, 24.54, 36.15 and 47.77 µM of BSA; (C) 2.8 x 10^{-5} M **L2** in the absence and presence of 0, 5.5, 13.5, 27.1, 40.0 and 52.6 µM of BSA; (D) 2.9 x 10^{-5} M **C2** in the absence and presence of 0, 12.86, 25.28, 37.27, 48.87 and 60.07 µM of BSA in buffered solution (10 mM, PBS pH 7.4)

3.3.2 Circular dichroism spectroscopy

Circular Dichroism (CD) spectroscopy is recognized as an important technique to explore the conformational alteration of the secondary structure of proteins [**46**]. To determine the structural changes of BSA by the addition of Schiff base complexes, we measured the CD spectra to investigate possible conformational changes of serum albumins in solution. The technique is appropriate because BSA has a high percentage of α-helical structure, which shows a characteristic CD signal in the far-UV region [**35**]. It is worthwhile to note that the studied ligands and complexes do not possess any CD spectra under the investigated wavelength range 200-280 nm, or any other, as they are not chiral. Here the spectra are solely due to the protein

and characterized by two negative bands at 210 and 220 nm due to π→π* and n→π* transitions in the peptide bonds of α-helix, respectively [**47**]. The effect of the complexes on the secondary structure of the protein was studied by keeping the concentration of BSA at 1×10^{-6} M while varying the concentration of Schiff base complexes **C1** and **C2,** in a buffer solution (10 mM PBS, pH 7.4) up to 3:1 molar ratio of compound: BSA as shown in **Fig. 13**.

Upon addition of the Schiff base metal complexes, the CD spectra of the protein undergo a gradual decrease in band intensity of both negative bands without any significant shift of the peak positions. This phenomenon indicates the progressive reduction of the α-helical content due to interaction with the probes. The effect is stronger for complex **C1** than **C2**.

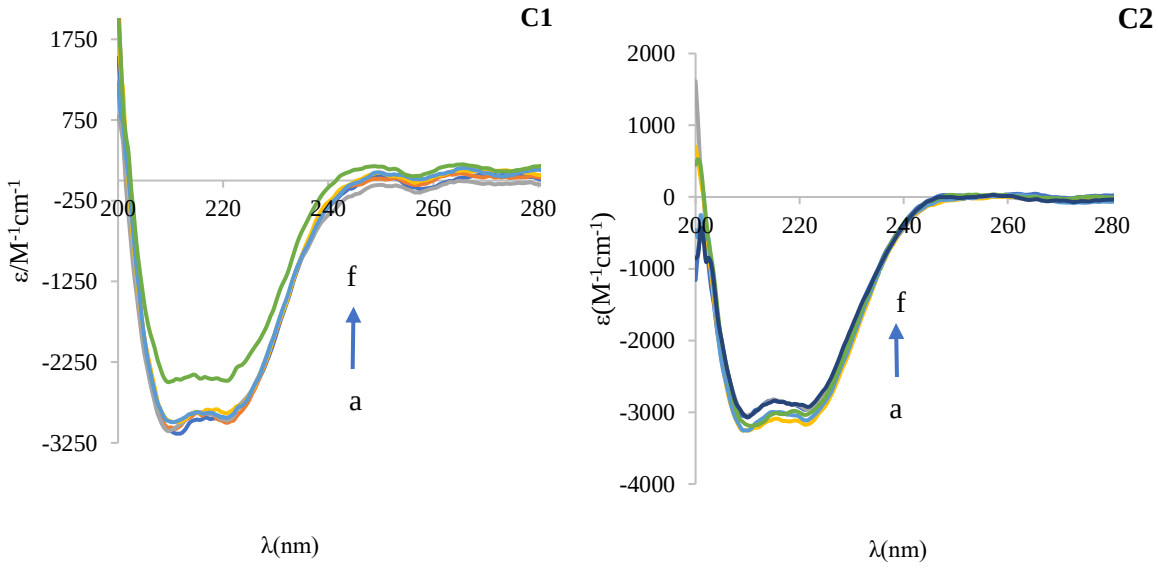

Figure 13 CD spectra of BSA in the absence and presence of increasing concentrations of **C1** and **C2**. [BSA] = 1.0×10^{-6} M where the concentration ratios of BSA: compounds (a–f) were: 1:0; 1:0.5; 1:1; 1:1.5; 1:2; and 1:3.

3.3.3 Fluorescence quenching

Albumin is a water-soluble protein, which is crucial for many living organisms. The significant role of transporting essential trace metal ions, metal complexes, and drugs in the circulatory system is played by albumin [**62**, **63**]. One useful technique to study binding of a compound to albumin is fluorescence. Protein fluorescence is generally due to three amino acids, namely tyrosine (Tyr), tryptophan (Trp-134, located on the surface of domain IB, Trp-212 located in the hydrophobic pocket of domain IIA) and phenyl alanine (Phe) residues. Thus, BSA fluorescence emission spectra were recorded in the absence and presence of increasing

concentrations of complexes to investigate its binding to BSA. BSA solutions show strong fluorescence emission having its maxima at 345 nm upon excitation at 285 nm, which is associated with tryptophan residues, (**Fig. 14**). The fluorescence intensity was strongly quenched upon increasing the Schiff base ligands and complex concentration whereas no changes were observed in the position of the emission maximum wavelength and peak shape. As a result, we can conclude that the complexes bind BSA, which results in conformational changes in the secondary structure of the protein and quenching of its intrinsic fluorescence [**64**].

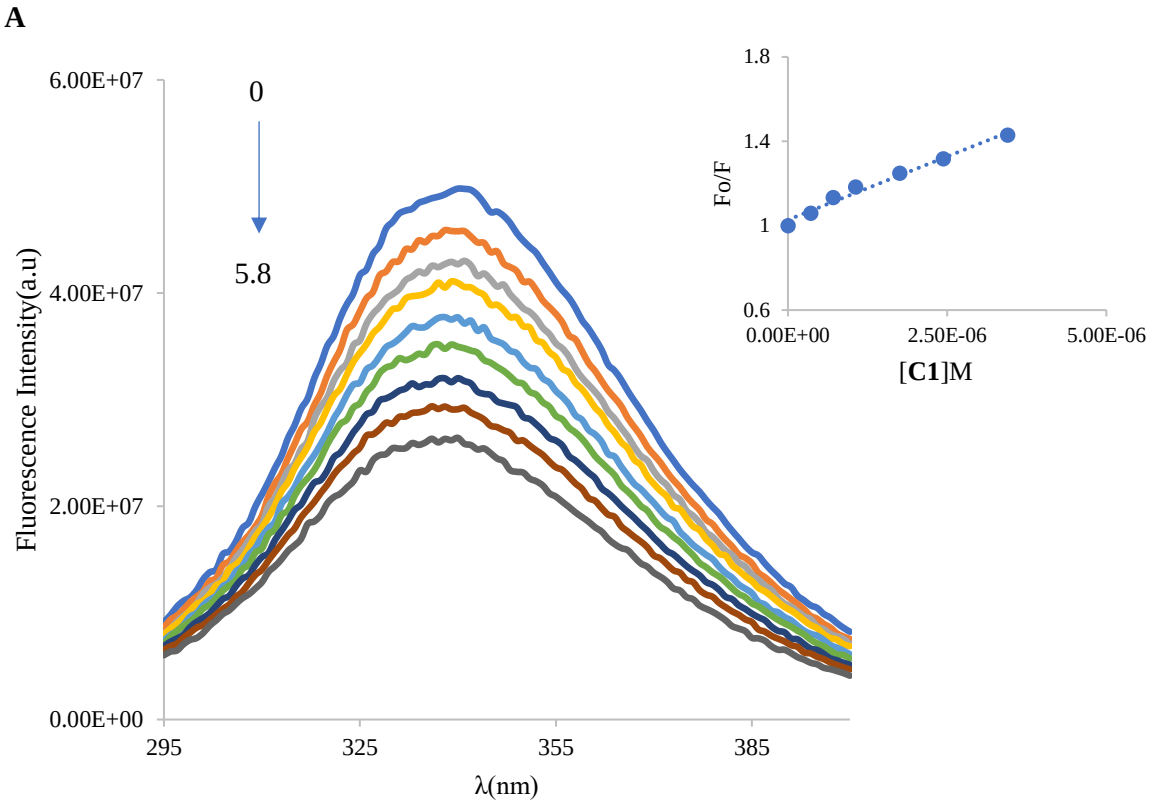

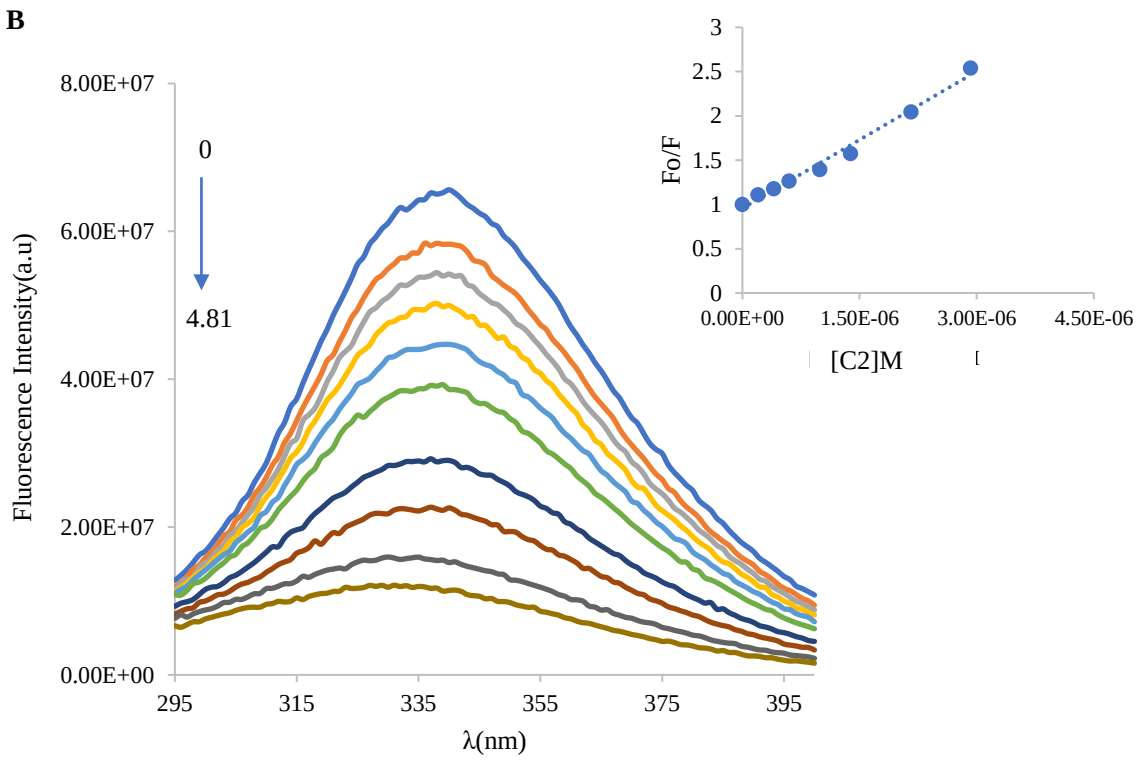

Figure 14 Fluorescence emission spectra of BSA in absence and presence of different concentrations of **C1** (A) and **C2** (B) at room temperature where [BSA] = 1.25× 10^{-6} M and [compound] varied from 0 – 5.8 × 10^{-6} M (for **C1**) and 0 – 4.81 × 10^{-6} M (for **C2**). Arrows show changes upon increasing complexes concentration. Inset: Stern-Volmer plots of $\mathbf{F_0/F}$ *vs.* [Complex].

The mechanism by which collisional encounters between the fluorophore and quencher take place is referred to as quenching. There are two main methods for BSA fluorescence quenching; static and collisional or dynamic quenching, which are a valuable source of information regarding binding between the fluorescent sample and the quencher. The quenching can be described by the linear Stern–Volmer equation.

$$F_0/F = 1+K_{sv}[Q] = 1+K_q\tau_0[Q] \qquad (\mathbf{1})$$

Where F and F_0 are BSA fluorescence intensities in the presence and absence of quencher (metal complexes), respectively. K_q, K_{sv}, τ_0 and [Q] are the quenching rate constant, the Stern-Volmer quenching constant, the average biomolecule lifetime in the absence of quencher and the quencher concentration, respectively. K_{sv} values at 298 K were found to be in the range of 10^4 - 10^5 M^{-1} (see **Table 8)**. These constants indicate that BSA has high binding affinity for these compounds. The K_q values, were calculated considering τ_0= 10^{-8} s, [**65**] and are all greater than the maximum scatter collision quenching constant of quenchers with BSA

(2×10^{10} M^{-1} s^{-1}) [**66**] suggesting a static quenching mechanism [**67**], resulting from the formation of an adduct between the protein and the Zn-complexes.

Table 8 Parameters determined in the fluorescence quenching studies.

	L1	**C1**	**L2**	**C2**
$\mathbf{K_{SV}}$ / $\mathbf{M^{-1}}$	6.10×10^4	1.20×10^5	4.51×10^5	5.15×10^5
$\mathbf{K_q}$ / $\mathbf{M^{-1}s^{-1}}$	6.10×10^{12}	1.20×10^{13}	4.51×10^{13}	5.15×10^{13}
$\mathbf{K_a}$ / $\mathbf{M^{-1}}$	1.97×10^5	2.36×10^3	9.81×10^5	2.38×10^6
N	1.1	0.70	0.99	1.2

3.3.3.1 Determination of binding constant and the number of binding sites

The following equation (**Eqn. 2**) can be used to calculate the binding constant (K_a) and the number of binding sites (n) for the static quenching interaction, assuming similar and independent binding sites in the biomolecule:

$$\log(F_0\text{-}F)/F = \log K_a + n\log[Q] \qquad (\mathbf{2})$$

where n is the average number of binding sites per albumin molecule and K_a is the binding constant in the protein complex interaction. The double logarithmic plot of log $[(F_0 - F)/F]$ versus log[Q] is shown in **Fig. 15**. The K_a and n values, calculated at 298 K, are included in **Table 8.** Values between 10^3 and 10^6 M^{-1} were obtained for K_a indicating weak to strong binding to BSA where n values of *ca.* 1 imply only a binding site in each albumin. **C2** shows a much higher binding constant than **C1**, and the complex **C2** show higher binding ability than its ligand, **L2**.

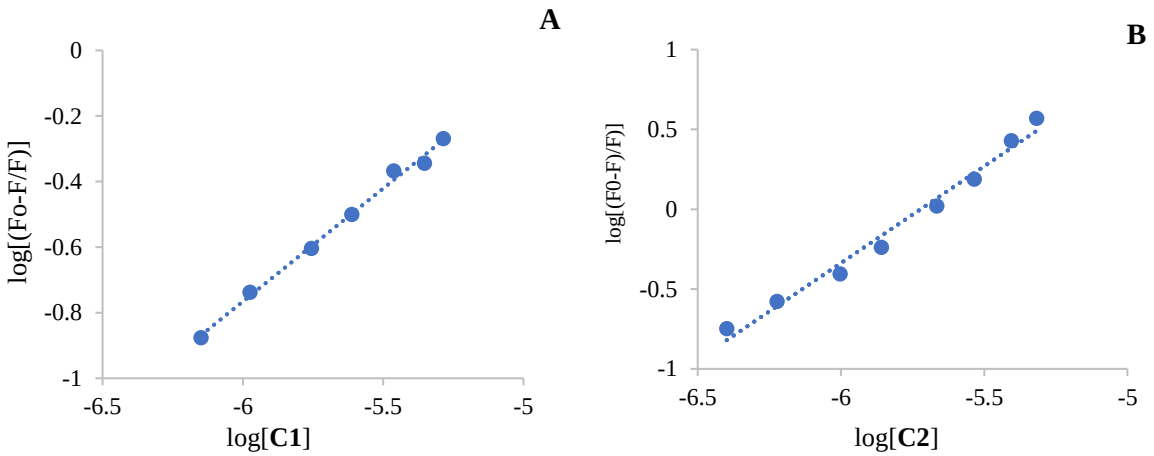

Figure 15 Scatchard plots of log [($\mathbf{F}_0 - \mathbf{F}$)/**F**] vs. log [**Q**] for determination of the complex-BSA binding constant and the number of binding sites on BSA for **C1** (A) and **C2** (B).

3.4 DNA binding affinity

3.4.1 Absorption spectroscopic measurements

The interaction between metal complexes and DNA is commonly studied by electronic absorption spectroscopy since binding to the macromolecule leads to changes in the electronic spectrum [**68**]. Hypochromism and bathochromism generally occur by the intercalation of metal complexes to DNA due to strong π–π* stacking interactions between the aromatic chromophore of the complex and the DNA base pairs [**69, 70**]. Hyperchromism in absorption intensity is usually caused by minor groove binding of complexes to DNA, which indicates the unwinding of the DNA double helix and its unstacking and the concomitant exposure of the bases [**71, 72**]. **Fig. 16** shows the electronic absorption spectra of the complexes in the absence and presence of *ct*DNA. The spectra mainly consist of intraligand and ligand-to-metal charge transfer (LMCT) π → π* and n → π* transition bands centred at 296, 350 and 422 nm for complex **C1** and 390 and 465 nm for **C2**. The addition of increasing amounts of DNA (up to [DNA]/[complex] = 4.0) significantly changes the UV–vis absorption spectra. Decreased absorption intensity (hypochromism) and slight increase in absorption wavelength (bathochromism) for both complexes confirms the binding of complexes to DNA by intercalation and formation of new complex adducts with double helical *ct*DNA.

To elucidate and compare the binding strength of the four compounds with *ct*DNA quantitatively, the results were fitted assuming the formation of a 1:1 association complex between DNA and the compounds,

$$C_{px} + DNA \leftrightarrows C_{px}:DNA \qquad K_a = \frac{[Cpx:DNA]}{[Cpx][DNA]}$$

The total concentration of DNA and compounds are the sum of the concentrations of free and associated forms, respectively,

$$C_{DNA} = [DNA] + [Cpx:DNA] \quad (3)$$

$$C_{Cpx} = [Cpx] + [Cpx:DNA] \quad (4)$$

and these can be used to rewrite the concentration of associated form as a function of the total concentrations, C_{DNA} and C_{Cpx}, and of the binding constant, K_a,

$$[Cpx:DNA] = \frac{1}{2}\left(C_{DNA} + C_{Cpx} + \frac{1}{K_a}\right) - \frac{1}{2}\sqrt{\left(C_{DNA} + C_{Cpx} + \frac{1}{K_a}\right)^2 - 4 \cdot C_{DNA} \cdot C_{Cpx}} \quad (5)$$

The apparent molar absorptivity of a given solution of a compound and DNA is obtained from the molar fraction average of the molar absorptivity of the individual species,

$$\bar{\varepsilon}^{\lambda} = \frac{[Cpx]}{C_{Cpx}}\varepsilon^{\lambda}_{Cpx} + \frac{[Cpx:DNA]}{C_{Cpx}}\varepsilon^{\lambda}_{Cpx:DNA} \quad (6)$$

The experimental results were fitted using equations 4, 5 and 6 by adjusting the values of molar absorptivity of the individual species $\varepsilon^{\lambda}_{Cpx}$and $\varepsilon^{\lambda}_{Cpx:DNA}$ at each wavelength selected and the value of the binding constant, K_a, for each compound studied. Upon fitting the data, the intrinsic binding constants (K_a) were found to be 4.77×10^3, 2.94×10^4, 7.74×10^5 and 2.73×10^3 for **L1**, **L2**, **C1** and **C2**, respectively. **C1** has higher binding constant than its Schiff base ligand, **L1**, where coordination with zinc improved the binding of the compound with DNA, whereas, **C2** has lower binding constant than **L1**. Moreover, it is apparent that **C1** has much higher affinity than **C2** due to presence of two aromatic pyridines, which are hydrophobic and easily insert itself between DNA base-pairs through a combination of π–π stacking and hydrophobic interactions [**73**].

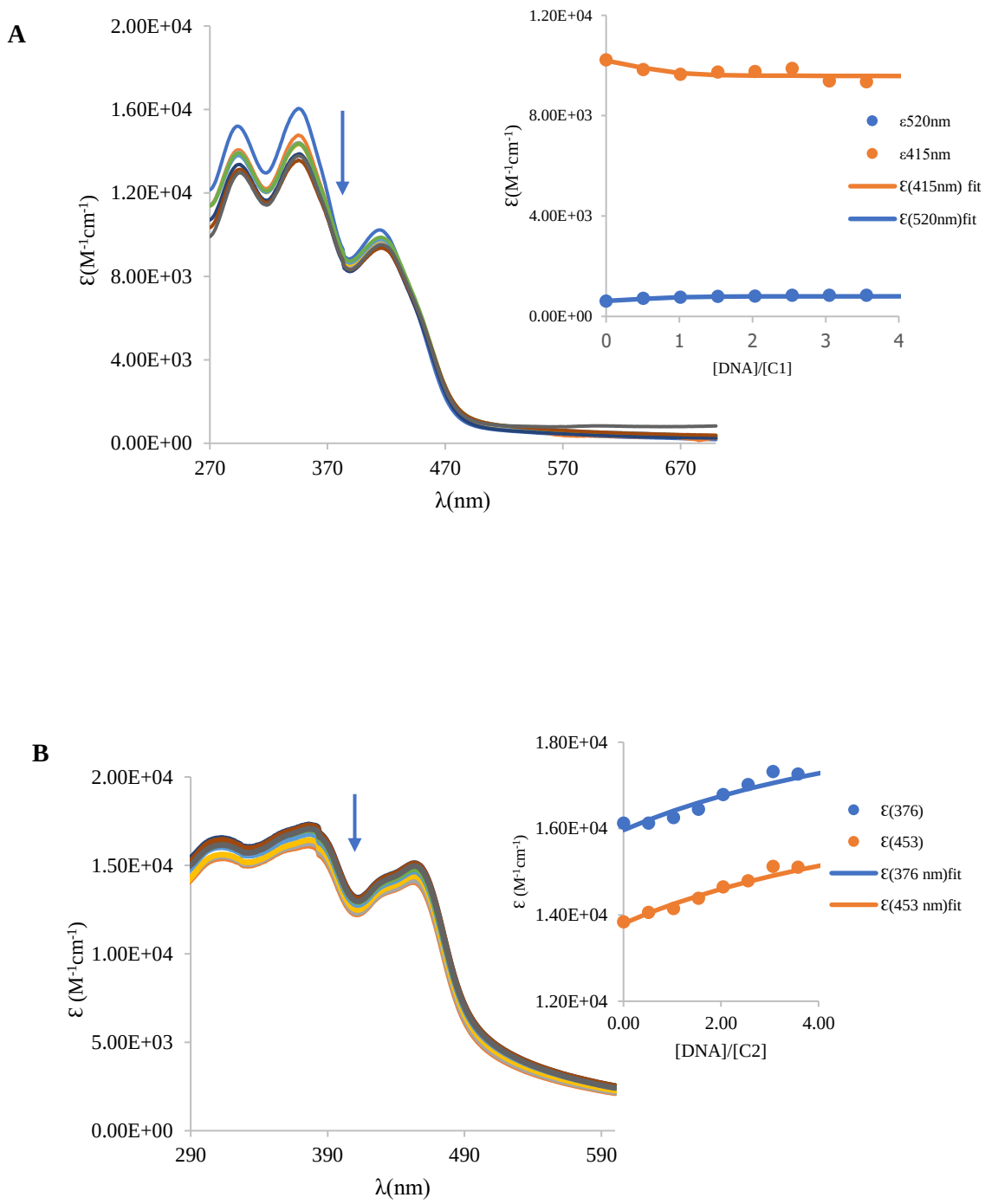

Figure 16 Electronic spectra of complexes in buffer solution (PBS, 10 mM, pH 7.4) upon increasing of DNA concentration, ranging from 0 to 8.2×10^{-5} M and 0 to 5.6×10^{-5} M for **C1** and **C2** respectively. [**C**omplex] = 2.6×10^{-5} and 2.5×10^{-5} M for **C1** and **C2** respectively. Inset: Variation of the molar absorptivity at wavelengths at 296, 350 and 422 nm for **C1** and 390 and 465 nm for **C2** with [DNA]/[Complex] ratio where the lines show the fitted model to determine the binding constant of the complex with DNA.

3.4.2 Circular dichroism experiments

Circular Dichroism (CD) is one of the best techniques to investigate the conformational changes and morphology of DNA [**74**]. CD spectroscopy is based on the differences between the levorotatory and dextrorotatory polarized light absorptions [**75**]. There are two characteristic bands of B type DNA in CD spectra (**Fig. 17**). The positive band, at 275 nm, corresponds to π–π* interaction of bases and the negative one, at 245 nm, is associated with the dextrorotatory helix structure [**76**]. These bands are very sensitive to the DNA interactions with other molecules and depend on the interaction type. Covalent and intercalative binding are generally well known for affecting the DNA tertiary structure and lead to changes in the CD spectra of DNA, whereas less or no perturbation is shown by external binding modes (electrostatic interaction or groove binding) on the base stacking and helicity bands [**77**].

A

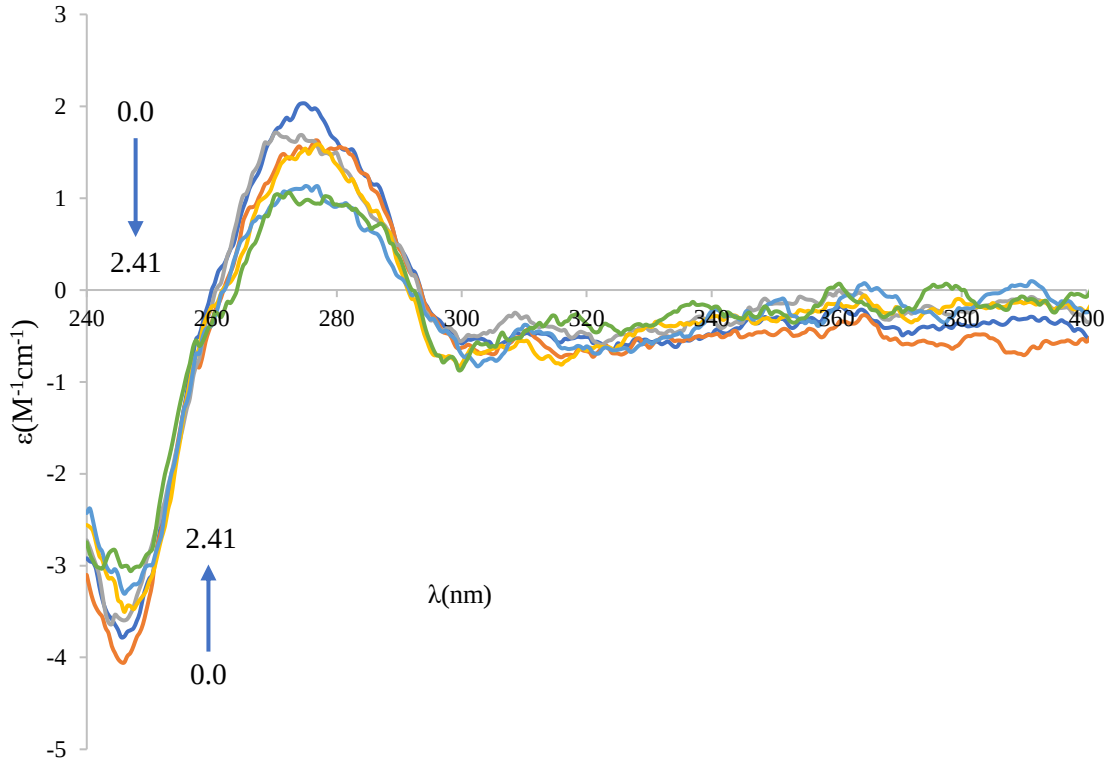

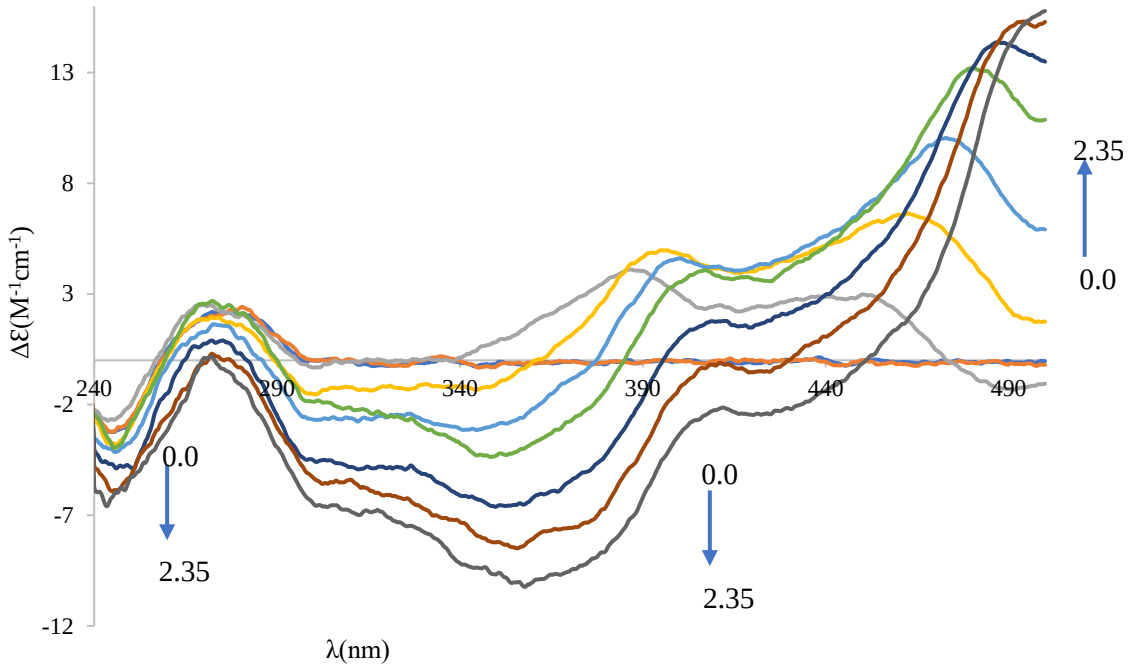

Figure 17 CD spectra of *ct*-DNA (6×10^{-5} M) in the absence and presence of increasing molar ratio of [complex]/[*ct*-DNA] ranges from 0:1 to 1:3.01 and 0:1 to 1:2.35 for **C1** (A) and **C2** (B), respectively, in buffered solution (PBS, 10 mM pH = 7.4).

In this experiment, successive addition of complexes from 0 to 8.2×10^{-5} M and 0 to 5.6×10^{-5} M for **C1** and **C2,** respectively, increases the ellipticity of the positive band at 275 nm where maximum molar ratio = 4.0 has been reached. For **C2** induced circular dichroism bands develop above 290 nm, being a clear indication of the interaction of **C2** with DNA. The two complexes can intercalate into DNA base stacking while the characteristics of the B form CD spectrum is still conserved, according to the results. In addition, the arrangement of the DNA bases is somewhat altered. Binding of the complexes does not cause significant changes in the helix conformation of *ct*-DNA since no clear variations are observed in the negative band [**78**]. The mode of interaction between the complex and DNA must be intercalative, according to the results [79, **80**].

3.5 In *vitro* biological activity studies

3.5.1 Cytotoxic activity

The *in vitro* cytotoxicity of **L1** and **L2** were evaluated on three cell lines (Caco-2, MCF-7 and PC-3) and one normal cell, NHDF. Under the same experimental conditions, fluorouracil (5FU) was used as a positive control. The activity was measured after 48 h incubation and IC_{50} values for tested compounds and the positive control against the cell lines are listed in **Table 9**. It is

worthwhile to mention that **L1** shows higher cytotoxicity towards most cells than 5FU. When we compare the IC_{50} values, it can be found that the IC_{50} values of **L1** are higher than that of **L2** for all the cancer cell lines, indicating that **L1** possessed better activities than **L2** under identical experimental conditions, however, both of tested compounds show no selectivity towards cancer cells.

Table 9 Cytotoxicity of the ligands (IC_{50} values in μM at 48h incubation) as well as the positive control, 5-FU, in Caco-2, MCF-7, PC-3 and NHDF cells.

	Caco-2	**MCF-7**	**PC-3**	**NHDF**
L1	3.98	1.36	2.92	1.41
L2	12.58	14.94	9.73	4.58
5-FU	0.82	4.93	3.30	17.00

3.5.2 Antimicrobial activity

The antibacterial and antifungal efficacy of the ligands and one Zn complex, **C1**, were tested against several strains of bacteria and two candida fungi and the results are presented in **Table 10**. The results obtained for antimicrobial activity of the compounds showed that **L1** is active against *L. monocytogenes*; **L2** is active against *K. pneumoniae*, *A. baumannii* and *S. aureus* and **C1** against *L. monocytogenes* and *S. aureus*. The ligand **L2** showed better activity against tested microbials compared to the other ligand and its metal complex. This higher activity is possibly due to interference in the normal cell process of the organism caused by the formation of hydrogen bonds through the azomethine group with the active centre of cell constituents [**81**]. Precise observation reveals that the compounds are less active against *P. aeruginosa* and *C. tropicalis* while more active against *L. monocytogenes* and *S. aureus*. **C1** showed improved activity against *S. aureus* compared to its free ligand and this enhanced activity of the complex may be attributed to chelation of Schiff base with metal ions that provide stability and more susceptibility against the bacterial pathogen [**82**, **83**]. It has been suggested that the structural components possessing additional (C=N) bond with nitrogen and oxygen donor systems inhibit enzyme activity due to their deactivation by metal coordination. This permits their efficient permeation through the lipid layer of organisms and destroys their activity [**84**]. The lower antibacterial activity of metal complexes may be due to strong interaction between the imine moieties and the metal ions. This type of interaction reduces the activity of imine moieties

toward inhibition of bacterial activities whereas the ligand has higher antibacterial activity than its metal complexes [**85**, **86**].

Table 10 Inhibition halo (mm) and minimum inhibitory concentration MIC (µg/mL) for different strains of bacteria and fungi.

Inhibition halo (mm)							
Compounds	***Klebsiella pneumoniae* ATCC 13883**	***Acinetobacter baumannii* LMG 1025**	***Listeria monocytogenes* LMG 16779**	***Pseudomonas aeruginosa* ATCC 27853**	***Staphylococcus aureus* ATCC25923**	***Candida albicans* ATCC 90028**	***Candida tropicalis* ATCC 750**
L2	6.0±0.0	6.0±0.0	6.0±0.0	6.0±0.0	11.6±0.2	6.0±0.0	6.0±0.0
L1	6.0±0.0	6.0±0.0	6.0±0.0	6.0±0.0	6.0±0.0	6.0±0.0	6.0±0.0
C1	6.0±0.0	6.0±0.0	6.7±0.6	6.0±0.0	7.2±0.1	6.0±0.0	6.0±0.0
MIC (µg/mL)							
L2	16	16	>64	>64	8	64	>64
L1	>64	>64	8	>64	64	>64	>64
C1	>128	>128	16	>128	16	>128	>128

4. Conclusions

In the current work Schiff base ligands derived from pyridin-2-yl-hydrazonomethyl phenol and methyl-phenol-di-S-methyl dithiocarbazate were synthesized from the condensation of 2, 6-diformyl-4-methylphenol with 2-hydrazino pyridine and S-methyl carbazate. Both ligands were obtained in good yields and fully characterized by a set of analytical techniques, verifying the proposed structures.

The Zn(II) complexes (**C1**, **C2**) were synthetized by stirring ethanolic solutions of ligands and $Zn(CH_3COO)_2.2H_2O$. ^{1}H and ^{13}C NMR experiments were done for all ligands and zinc complexes in addition to elemental analysis and other spectroscopic techniques. The characterization suggests that the Schiff base **L2** coordinates the two metal ions through the phenolate-O, the imine-N and sulphur atom in the thiol form, while in **C1** the S atom is replaced by the pyridinic nitrogen. Acetate ions complete the coordination sphere in both complexes, yielding neutral Zn-complexes.

The stability of the compounds in buffered aqueous media (5 % DMSO and 95 % PBS) was evaluated and all are stable at least for three hours. The two Zn(II) complexes were tested for their biomolecule binding abilities such as serum albumin and nucleic acid. Various spectroscopic techniques were employed to investigate possible interactions of the compounds with these biomolecules. The results indicated that there is medium to moderate interaction between the complexes and biomolecules.

Results of biological studies against bacteria and fungi revealed moderate activity of the synthesized compounds, however, the results of cytotoxicity study showed that the tested compounds are cytotoxic both on cancer and normal cell lines.

In general, both families of compounds show potential to proceed further for biological studies to allow their development as metallodrugs, particularly the Methyl-phenol-di-S-methyl dithiocarbazate Zn(II) compound.

References

1. Sartaj T., Ahmad A., Farukh A., Mohd. A., Vivek B. Synthesis and characterization of copper(II) and zinc (II) - based potential. *Eur. J. Med. Chem* **2012**; 58, 308-316.

2. Chandraleka S., Ramya K., Chandramohan G., Dhanasekaran D., Priyadharshini A., Panneerselvam A. Antimicrobial mechanism of copper (II) 1,10 phenanthroline and 2,2'bipyridyl complex on bacterial and fungal pathogens. *J. Saudi. Chem. Soc.* **2011**; doi: 10.1016/j.jscs.2011.11.020.

3. Katja DM. and Chris O. Metallodrugs in medicinal inorganic chemistry. *Chem. Rev*. **2014**; 114, 4540 −4563.

4. Muthusamy S. and Natarajan R. Pharmacological activity of a few transition metal complexes: A short review. *J. Chem. Bio.Ther*. **2016**; 1(2), 1-17.

5. Mariya DM., Iyyam PS., Subramanian S., Pradeepa S., Damodar KS. Synthesis, spectroscopic characterization and DNA interaction of schiff base Cu(II), Ni(II) and Zn(II) complexes. *Int. J. Inorg. Bioinorg. Chem*. **2014**; 4(4), 61 - 67.

6. Chung HL., Sheng L., Hai JZ. and Dik LM. Metal complexes as potential modulators of inflammatory and autoimmune responses. *Chem. Sci.* **2015**; 6, 871–884.

7. Rezvania AR., Saravania H. and Hadadzadeh H. Synthesis, crystal structure, electrochemical and fluorescence studies of a novel Zn(II)-fluorophore, 1,10-phenanthroline-5,6-dione (phendione). *J. Iran. Chem. Soc.* **2010**; 7(4), 825-833.

8. Wang L., Liang N. and Jia Y. Syntheses, structures, fluorescent properties and natural bond orbital analyses of metal–organic complexes based on 5,6-substituted 1,10-phenanthroline derivatives. *Polyhedron* **2013**; 59, 115–123.

9. Hernández-Molina R. and Mederos, A. Comprehensive Coordination Chemistry II Elsevier Ltd, **2003**; 411.

10. Anand P., Patil VM., Sharma VK., Khosa RL. and Masand N., Schiff bases: A Review on Biological Insights. *Int. J. Drug Design Dis.* **2012**; 3, 851

11. Gupta KC., Sutar AK. and Lin CC., Polymer-supported Schiff base complexes in oxidation reactions. *Coord. Chem. Rev.*, **2009**; 253, 1926.

12. Gupta KC. and Sutar AK., Catalytic activities of Schiff base transition metal complexes. *Coord. Chem. Rev.*, **2008**; 252, 1420.

13. Al Zoubi W. Solvent extraction of metal ions by use of Schiff bases *J. Coord. Chem.*, **2013**; 66, 2264.

14. Pfeiffer P., Breith E., Lübbe E. and Tsumaki T., Tricyclische orthokondensierte Nebenvalenzringe *Justus Liebig's Annalen der Chemie*, 1933; 503, 84.

15. Atkins R., Brewer G., Kokot E., Mockler GM. and Sinn E., Copper(II) and nickel(II) complexes of unsymmetrical tetradentate Schiff base ligands *Inorg. Chem.*, **1985**; 24, 127.

16. Campbell KN., Sommers AH. and Campbell BK., Preparation of unsymmetrical secondary aliphatic amines, *J. Am. Chem. Soc.*, **1944**; 66, 82

17. Hine J. and Yeh CY., Equilibrium in formation and conformational isomerization of imines derived from isobutyraldehyde and saturated aliphatic primary amines *J. Am. Chem. Soc.*, **1967**; 89, 2669.

18. Savich IA., Pikaev AK., Lebedav IA. and Spitsyn VI. Synthesis and antimicrobial activities of Schiff bases derived from 5-chloro-salycylaldehyde. *Vestnik. Moskov. Univ*, **1956**; 11, 225.

19. Tazoki H. and Miyano K. Synthesis, characterization, antibacterial studies of Co(II), Ni(II) and Zn(II) complexes of some Schiff base ligands *J. Am. Chem. Soc.*, **1959**; 9769.

20. Brewster CM. Schiff's bases from 3,5-dibromo-salicylaldehyde, *J. Am. Chem. Soc.*, **1924**; 46, 2463.

21. Sayer JM., Pinsky B., Schonbrunn A. and Washtien W. Mechanism of carbinolamine formation *J. Am. Chem. Soc.*, **1974**; 96, 7998.

22. Wothers P., Greeves N., Warren S. and Clayden *J., Organic Chemistry*, Oxford University Press, Oxford, 1st edn., **2001**; 348.

23. Banerjee, A. Guha, J. Adhikary, A. Khan, K. Manna, S. Dey, E. Zangrando, D. Das. Dinuclear cobalt(II) complexes of Schiff-base compartmental ligands: Syntheses, crystal structure and bio-relevant catalytic activities. *Polyhedron*, **2013**; 60, 102-109.

24. Guha, T. Chattopadhyay, ND. Paul, M. Mukherjee, S. Goswami, TK. Mondal, E. Zan grando, D. Das. Radical pathway in catecholase activity with zinc-based model complexes of compartmental ligands. *Inorg. Chem*., **2012**; 51, 8750-8759.

25. Housectrof CE. and Sharpe AG., *Inorganic Chemistry 2nd Edition*, Pearson Education Limited, England, 2nd edn., **2005**; 639.

26. Cotton FA. and Wilkinson G., Advanced Inorganic Chemistry, John Wiley & Sons, New York, 5th edn., **1988**.

27. Sun XX., Qi CM., Ma SL., Huang HB., Zhu WX., Liu YC. Syntheses and structures of two Zn(II) complexes with the pentadentate Schiff-base ligands. *Inorg. Chem. Commun.* **2006**;9:911–914.

28. Chisholm MH., Gallucci JC. and Zhen H., Three-coordinate zinc amide and phenoxide complexes supported by a bulky Schiff base ligand. *Inorg. Chem.*, **2001**; 40, 5051

29. Yang J., Yuan JW., Zha RH. and Zeng QF. Bis{2-[3-(dimethyl-amino)propyl-imino-meth-yl]-4,6-dihydro-seleno-phenolato}zinc(II). *Acta Cryst.* **2009**; 65, 1090.

30. Deshmukh AP., Akerkar VG. and Salunkhe MM., Catalytic activities of Schiff base transition metal complexes *J. Mol. Catal. A: Chem.*, **2000**; 153, 75.

31. Kumaran JS, Priya S, Muthukumaran J, Jayachandramani N, Mahalakshmi S, Synthesis, Characterization and Biological Studies of Cu(II), Co(II), Ni(II) and Zn(II) Complexes of Tetradentate Schiff Base Ligand, *J. Chem. Pharma Res.*, 2013; 5(7), 56.

32. Yan G., Wu R., Chang Y. and Kang D. Pharmacokinetics and bio-distribution of new Gd-complexes of DTPA-bis (amide) (L3) in a rat model. *J. Korean. Soc. Magn. Reson. Med.* **2013**; 17 (4), 259.

33. Zhang D., Luo G., Ding X. and Lu C. Review: Preclinical experimental models of drug metabolism and disposition in drug discovery and development. *Acta Pharm. Sin*. B **2012**; 2 (6), 549.

34. Leuner C. and Dressman J. Improving drug solubility for oral delivery using solid dispersions. *Eur. J. Pharm. Biopharm*. **2000**; 50, 47.

35. Mohammad MD., Urvashi S., Hammad A., Nikhat M., Shaeel A. AT. and Athar AH. Synthesis, electrocatalytic behavior and biological evaluation of trimetallic macrocyclic complex with two different bridging ligands. *Can. Chem. Trans*. **2015**; 3(2), 184.

36. Waseem AW., Zeid AO., Imran A., Kishwar S. and Ming FH. Copper(II), nickel(II), and ruthenium(III) complexes of an oxopyrrolidine-based heterocyclic ligand as anticancer agents. *J. Coord. Chem*. **2014**; 67(12), 2110.

37. Nevin T., Ercan B., Naki C. and Kenan B. Investigation of synthesis, structural characterization, antioxidant activities and thermal properties of Zn(II), Fe(II) and Mn(II) complexes with thiophene-carboxylate ligand. *J. Chem. Biochem*. **2015**; 3 (2), 13.

38. Ikechukwu PE. and Peter AA. Synthesis, characterization and biological studies of Metal(II) Complexes of (3E)-3-[(2-{(E)-[1-(2,4-Dihydroxyphenyl) ethylidene]amino}ethyl)imino]-1-phenylbutan-1-one Schiff Base. *Molecules*, **2015**; 20, 9788.

39. Floyd B., Jeffrey T., Jason W., Jacob D., Nikolay G., Antonio G. S. and Navindra P. S. Synthesis and structure of [(η6- p-cymene)Ru(2-anthracen-9-ylmethylene-Nethylhydrazinecarbothioamide) Cl]Cl; biological evaluation, topoisomerase II inhibition and reaction with DNA and human serum albumin. *Metallomics* **2011**; 3 (5), 491.

40. Wozniak K. and Blasiak J. Review: Recognition and repair of DNA-cisplatin adducts. *Acta Biochem.* **2002**; 49 (3), 583.

41. Maria DAM., Iyyam PS., Joel C., Biju BR., Subramanian S., and Damodar KS. Design, synthesis, characterization and DNA interaction of new Schiff base metal complexes. *J. Chem. Pharm. Res*. **2015**; 7 (11), 105.

42. Yong L., Zheng YY. and Ming FW. Synthesis, characterization, DNA binding Properties, fluorescence studies and antioxidant activity of transition metal complexes with hesperetin-2- hydroxy benzoyl hydrazone. *J. Fluoresc*. **2010**; 20, 891.

43. Peters T., Pulman FW., The plasma Proteins, Academic Press, **1975**; 133.

44. Gallagher S.R., Ausubel F.A., Brent R., Kingston R.E., Moore D.D., Seidman J.G., Smith J.A., Struhl K. (Eds.) Current Protocols in Molecular Biology, John Wiley & Sons, New York, **1989**.

45. Lakowicz JR., Principles of Fluorescence Spectroscopy, 2nd ed., Plenum Press, New York, **1999**; 237.

46. Quiming NS., Vergel RB., Nicolas MG., Villanueva JA. Interaction of bovine serum albumin and metallothionein *J. Health Sci.* **2005**; 51(1), 8

47. Kumar CV., Asuncion EH. DNA,binding studies and site selective fluorescence sensitization of an anthryl probe. *J. Am. Chem. Soc.*, **1993;** 115 (19), 8547.

48. Marmur, J. A Procedure for the Isolation of Deoxiribonucleic Acid from Microorganisms. *J. Mol. Biol.*, 1961; 3, 208.

49. Nassar AM, Hassan AM, Elkmasha AN, Ahmed YZ. Synthesis and characterization of novel binuclear complexes. *Int. J. Chem Biochem.* **2012**; 2:83.

50. Hassan AM, Nassar AM, Ahmed YZ, Elkmash AN. Synthesis, characterization and biological evaluation, of binuclear OF Fe(III), Co(II), Ni(II), Cu(II) and Zn(II) complexes with schiff base (E)-4-[(hydroxyl phenylimino)methyl]benzene-1, 2-diol. *Int. J. Pharm. Sci Res*. **2012**; 3(7):2243.

51. Chavan VL, Mehta BH. X-ray, thermal and biological studies of Ru(III), Rh(III) and Pd(II) schiff base metal complexes. *Res. J. Chem. Envt*. **2011**; 15(2):57.

52. Neelakantan MA, Esakkiammal M, Mariappan SS, Dharmaraja J, Jeyakumar T. Synthesis, characterization and biocidal activities of some schiff base metal complexes. *Indian J. Pharma. Sci*. **2010**; 72(2): 216.

53. Silverstein RM. and Webster FX., Spectrometric Identification of Organic Compounds, John Wiley and Sons, New York, NY, USA, 6th edition, **1997**.

54. Tumer M., Deligonul N., Golcu A., Akgun E., and Dolaz M., "Mixed-ligand copper (II) complexes: investigation of their spectroscopic, catalysis, antimicrobial and potentiometric properties," *Tran Metal Chem*. **2006**; 31(1): 1–12.

55. Mohammed IA. and Hamidi RM., "Synthesis of new liquid crystalline diglycidyl ethers," *Molecules,* **2012**; 17(1); 645.

56. Mounika K., Anupama B., Pragathi A., and Gyanakumari C., "Synthesis and characterization and biological activity of Schiff base derived from 3-ethoxy salicylaldehyde and 2-amino benzoic acid and its transition metal complexes," *J. Sci. Res.* **2010**; 2(3); 513.

57. Sabic AE., Karabork M., Ceyhan G., Tumer M., and Digrak M. "Polydentate schiff base ligands and their La(III) complexes: synthesis, characterization, antibacterial, thermal and electrochemical properties," *Int. J. Inorg Chem*. **2012**; Article ID 791219, 11 pages.

58. Latheef, L., & Prathapachandra Kurup, M. R. Spectral and structural studies of nickel (II) complexes of salicylaldehyde 3-azacyclothiosemicarbazones. *Polyhedron,* **2008**; *27*, 35.

59. Emara AA. "Structural, spectral and biological studies of binuclear tetradentate metal complexes of N_3O Schiff base ligand synthesized from 4,6-diacetylresorcinol and diethylenetriamine," *Spectrochimica Acta Part A*: *Mol. Biomol. Spect.,* **2010**; 77(1); 117.

60. Jadeja RN. and Parmar NJ., "Oxovanadium(IV), Cr(III), Fe(III), Fe(II), Ni(II), Cu(II), Zn(II), and UO_2(VI) chelates from onno donor Schiff base ligand," *Syn. React Inorg Metal-Org Chem*, **2005**; 35, 111.

61. Clayden, J., Greeves, N., Warren, S., and Wothers, P. Organic Chemistry, 1st ed.; Oxford University Press: Oxford, **2001**.

62. Zhang YZ, Zhang XP, Hou HN. Study on the interaction between Cu (phen)23þ and bovine serum albumin by spectroscopic methods, *Biol. Trace Elem. Res*. 121 (2008) 276–287.

63. Guo XJ, Zhang L, Sun XD. Spectroscopic studies on the interaction between sodium ozagrel and bovine serum albumin, *J. Mol. Struct.* 928 (2009) 114–120.

64. Nicholson JP, Wolmarans MR, Park GR. The role of albumin in critical illness. *Br. J. Anaesth.* **2000**;85 :599 – 610.

65. Lakowicz R., Weber G., Quenching of fluorescence by oxygen. Probe for structural fluctuations in macromolecules. *Biochem.,* **1973**;12(21), 4161–4170.

66. Bhat SS. , Kumbhar AA. , Heptullah H. , Khan AA. , Gobre VV. , Gejji SP. , Puranik VG. Synthesis, electronic structure, DNA and protein binding, DNA cleavage, and anticancer activity of fluorophore-labeled copper (II) complexes. *Inorg. Chem.* **2010**; 50, 545.

67. Tolosa, I. Gryczynski, LR. Eichhorn, JD. Dattelbaum, FN. Castellano, G. Rao, JR. Lakowicz Glucose sensor for low-cost lifetime-based sensing using a genetically engineered protein. *Anal. Biochem.*, **1999**; 267 ,114.

68. Solute perturbation of protein fluorescence. Quenching of the tryptophyl fluorescence of model compounds and of lysozyme by iodide ion. Biochemistry, **1971**; 10 , 3254.

69. Long E.C., Jacqueline K.B. On demonstrating DNA intercalation. *Acc. Chem. Res.* **1990**; 23(9), 271-273

70. Chen ZF, Shi YF, Liu YC, Hong X, Geng B, Peng Y, Liang H. TCM active ingredient oxoglaucine metal complexes: crystal structure, cytotoxicity, and interaction with DNA. *Inorg. Chem***. 2012**;51:1998–2009.

71. Abedi A., Lighvan ZM, Ostad SN. Cytotoxicity and DNA/BSA binding ability of copper(II) complexes with dimethyl bithiazole *Monatsh. Chem.* 2016; 147, 1651.

72. Tjioe L, Meininger A, Joshi T, Spiccia L, Graham B. Efficient plasmid DNA cleavage by copper(II) complexes of 1,4,7-triazacyclononane ligands featuring xylyl-linked guanidinium groups. *Inorg. Chem.* **2011**; 50(10): 4327-4339.

73. Avendaño C. and Menendez JC. Medicinal Chemistry of Anticancer Drugs, Elsevier B.V., Chapter 7: DNA intercalators and Topoisomerase inhibitors, **2008**; 199–228.

74. Kumar P.S. Gorai, M.K. Santra, B. Mondal, D. Manna. DNA binding, nuclease activity and cytotoxicity studies of Cu(II) complexes of tridentate ligands. *Dalton Trans*. **2012**; 41, 7573.

75. Rudra S., Dasmandal S., Patra C., Kundu A., Mahapatra A. Binding affinities of Schiff base Fe (II) complex with BSA and calf-thymus DNA: spectroscopic investigations and molecular docking analysis. *Spectrochim., Acta A.* **2016**; 166, 84.

76. Kelly, S.M., Price, N.C. The use of circular dichroism in the investigation of protein structure and function *Curr. Protein Pept. Sci*. **2001**; 1, 349.

77. Rajendran A., Nair B.U. Unprecedented dual binding behaviour of acridine group of dye: A combined experimental and theoretical investigation for the development of anticancer chemotherapeutic agents. *BBA-GEN Sub*., **2006**; 1760, 1794.

78. Wei Q., Dong J., Zhao P., Li M., Cheng F., Kong J., Li L. DNA binding, BSA interaction and SOD activity of two new nickel(II) complexes with glutamine Schiff base ligands. *J. Photochem. Photobiol.* **2016;** 161, 355-367

79. Shahrakia S, Mansouri-Torshizia H, Sori Nezamia Z, Ghahghaeib A, Yaghoubia F, Divsalarc A, Sabouryd AA, Shirazie FH. The effects of extending of co-planarity in a series of structurally relative polypyridyl Palladium(II) complexes on DNA-binding and cytotoxicity properties. *Iran. J. Pharm. Res.* **2014**;13, 1279–1294.

80. Chen Z.F., Liu Y.C. , Liu L.M., H.S. Wang, Qin S.H. , Wang B.L., Bian H.D., Yang B., Fun H.K., Liu H.G. Potential new inorganic antitumour agents from combining the anticancer traditional Chinese medicine (TCM) liriodenine with metal ions, and DNA binding studies. *Dalton Trans*. 2009; 262.

81. Joseyphus R. S., Nair M. S. Antibacterial and Antifungal Studies on Some Schiff Base Complexes of Zinc (II) *Mycobiology*. **2008**; 36(2), 93–98.

82. Al-Amiery A.A., Al-Majedy Y. K., Ibrahim H. H., Al-Tamimi A. A. Antioxidant, antimicrobial, and theoretical studies of the thiosemicarbazone derivative Schiff base 2-(2-imino-1-methyl imidazolidin-4-ylidene) hydrazine carbothioamide (IMHC). *Org. –Med. Chem. Lett*. **2012**; 2(4) doi: 10.1186/2191-2858-2-4.

83. Jesmin M., Ali M. M., Salahuddin M. S., Habib M. R., Khanam J. A. Antimicrobial Activity of Some Schiff Bases Derived from Benzoin, Salicylaldehyde, Aminophenol and 2,4 Dinitrophenyl Hydrazine. *Mycobiology*. **2008**; 36:70–73.

84. Bagihalli G. B., Avaji P. G., Patil S. A., Badami P. S. Synthesis, spectral characterization, in vitro antibacterial, antifungal and cytotoxic activities of Co(II), Ni(II) and Cu(II) complexes with 1,2,4-triazole Schiff bases. *Eur. J. Med. Chem*. **2008**; 43(12): 2639–2649.

85. Juh´asz L., Dinya Z., Antus S., and Gunda T.E. "A new approach for the synthesis of naturally occurring dihydrobenzo[b]furantype neolignans of potential biological activity," *Tetrahedron Lett*. **2000**; 41(14), 2491–2494.

86. Riyadh M. Ahmed, Enaam I. Yousif, and Mohamad J. Al-Jeboori, "Co (II) and Cd (II) Complexes Derived from Heterocyclic Schiff-Bases: Synthesis, Structural Characterisation and Biological Activity", *Sci. World J.* **2013**; Article ID 754868. https://doi.org/10.1155/2013/754868.

Appendices

A. NMR spectra

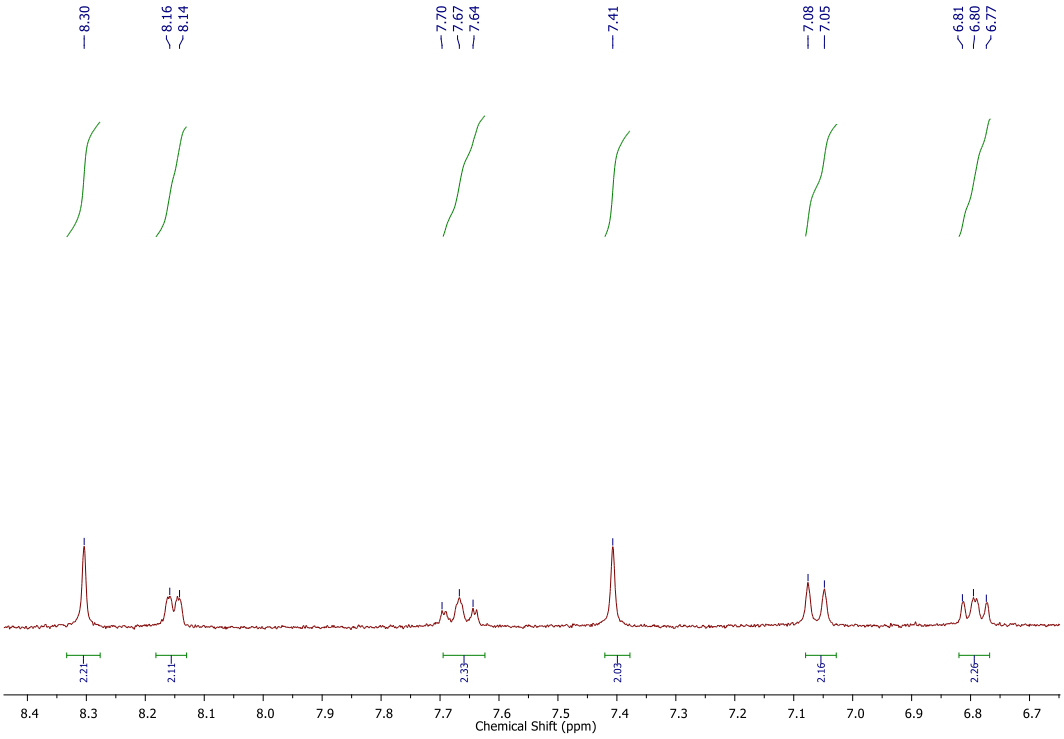

Figure A1 Aromatic region of the ^{1}H NMR spectrum of **L1** in DMSO-$_{d6}$ at room temperature.

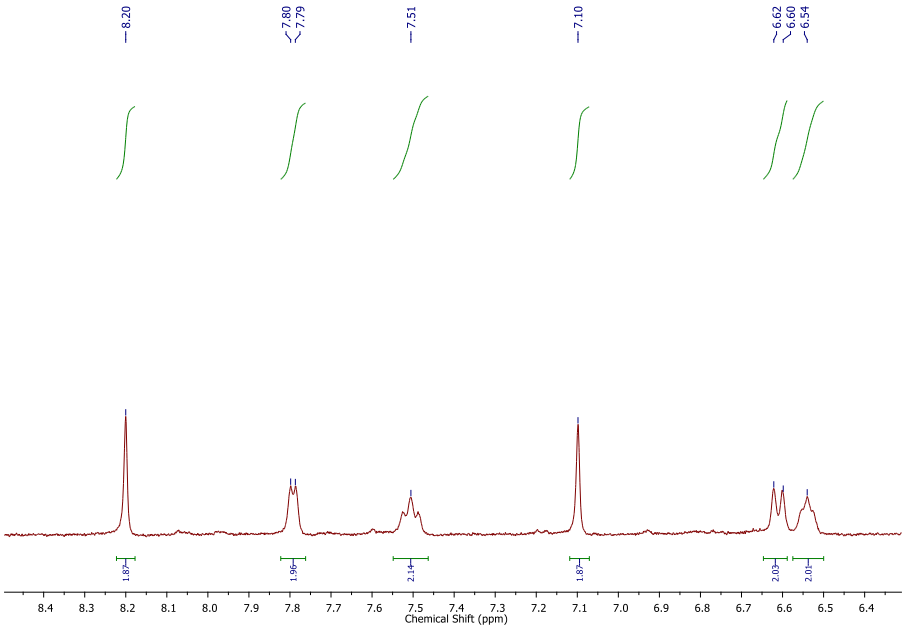

Figure A2 Aromatic region of the ^{1}H NMR spectrum of **C1** in DMSO-$_{d6}$ at room temperature.

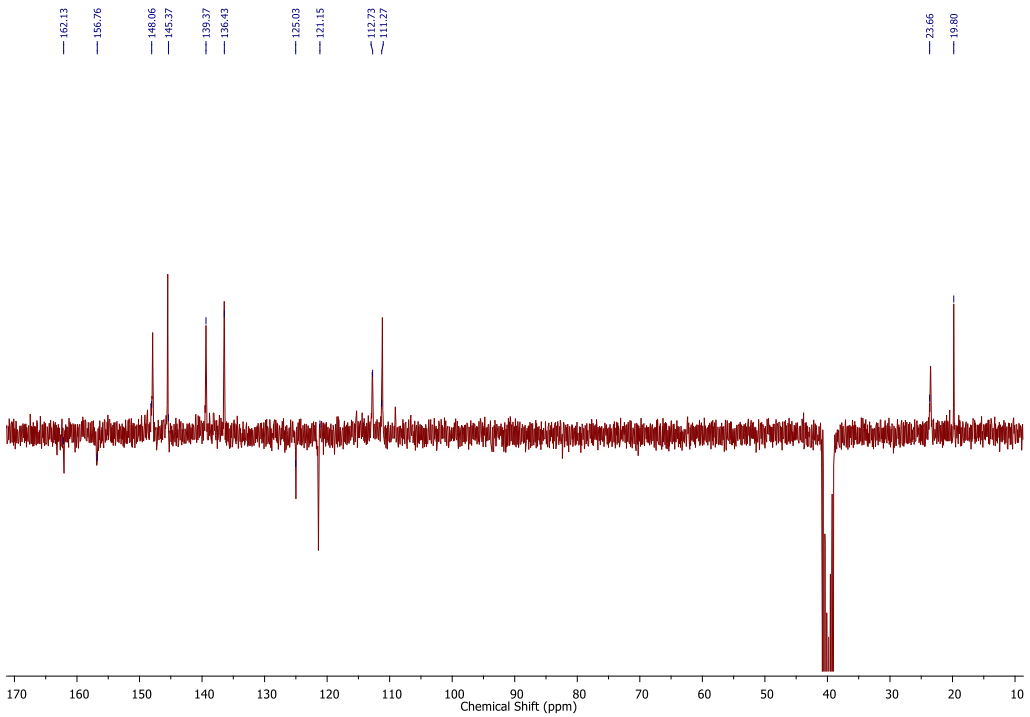

Figure A3 ^{13}C APT NMR spectrum of **C1**in DMSO-$_{d6}$ at room temperature.

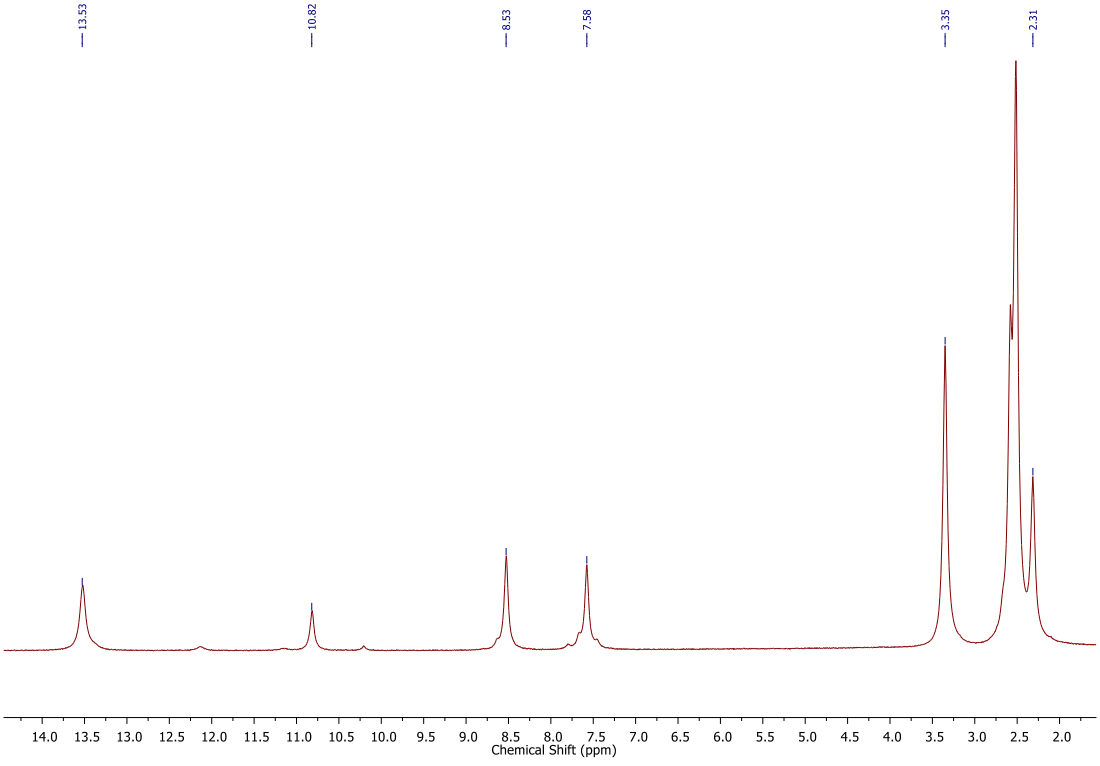

Figure A4 ^{1}H NMR spectrum of **L2** in DMSO-$_{d6}$ at room temperature.

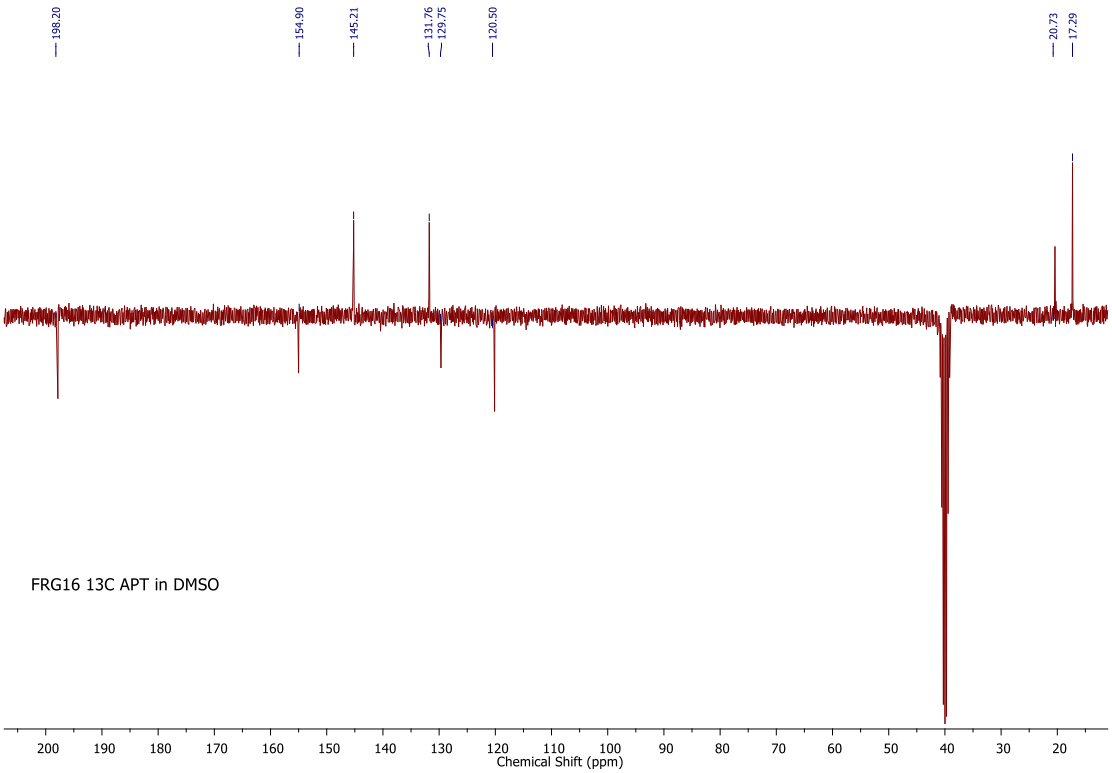

Figure A5 ^{13}C APT NMR spectrum of **L2** in DMSO-$_{d6}$ at room temperature.

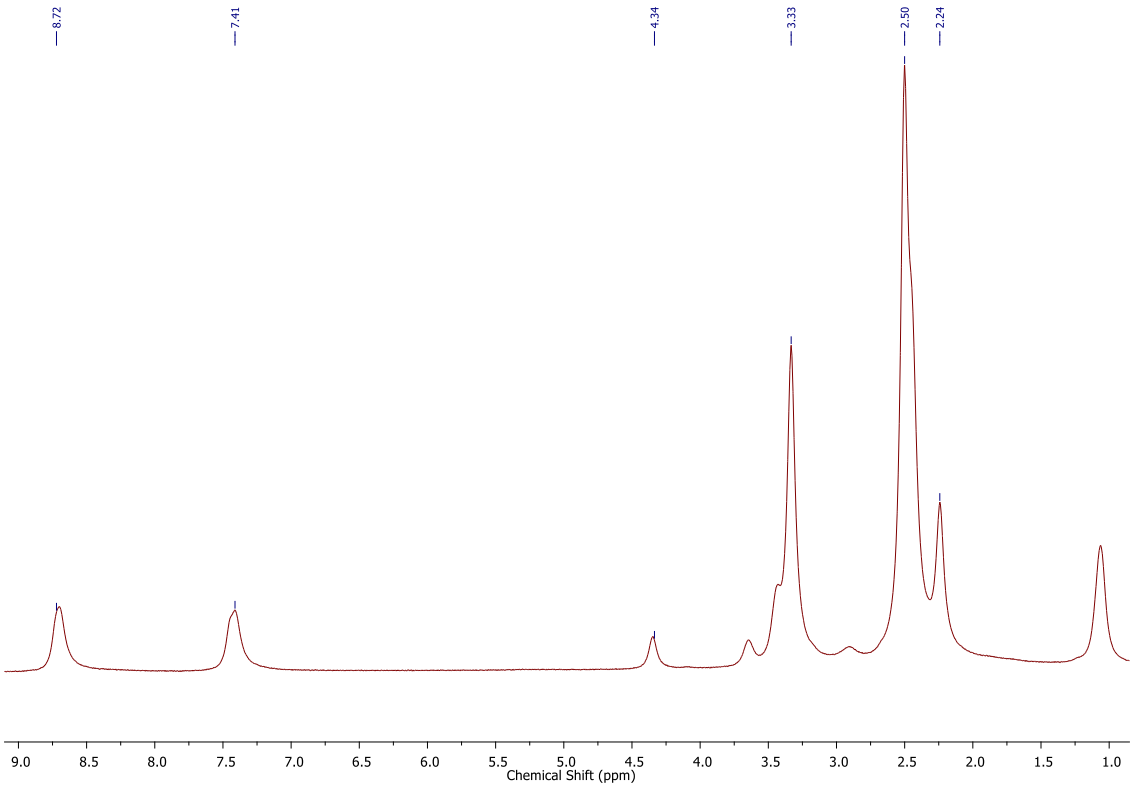

Figure A6 ^{1}H NMR spectrum of **C2** in DMSO-$_{d6}$ at room temperature

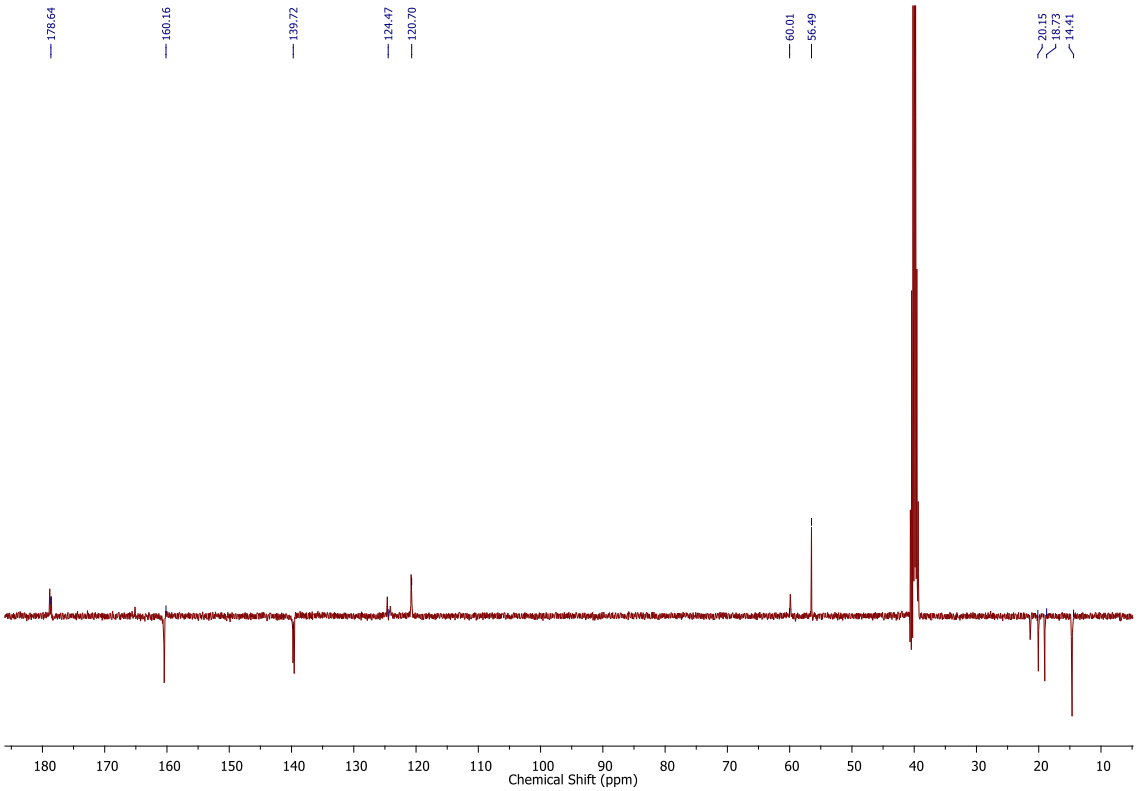

Figure A7 ^{13}C APT NMR spectrum of **C2** in DMSO-$_{d6}$ at room temperature.

B. FTIR Spectra

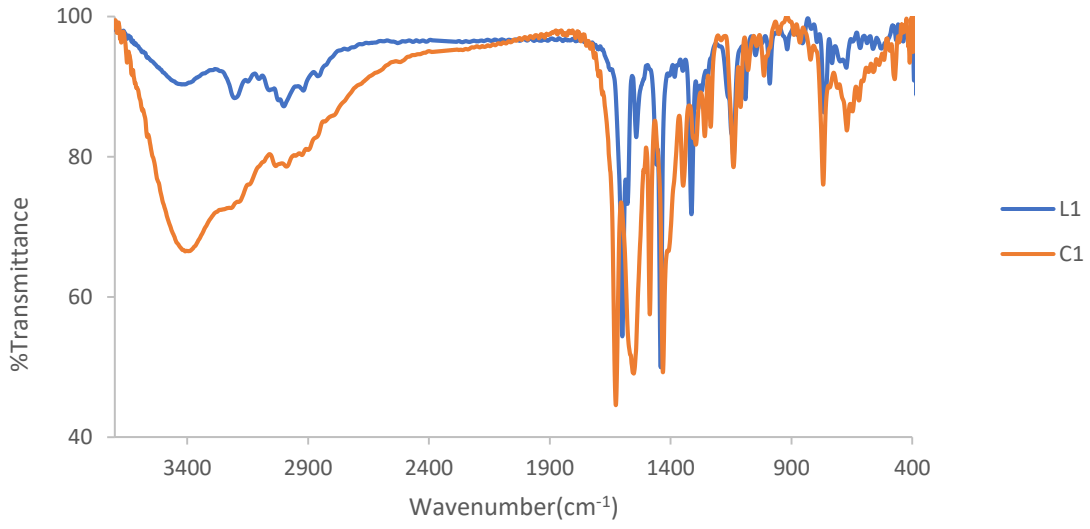

Figure C1 FTIR spectra for Schiff base ligand, **L1** and zinc complex, **C1** in KBR.

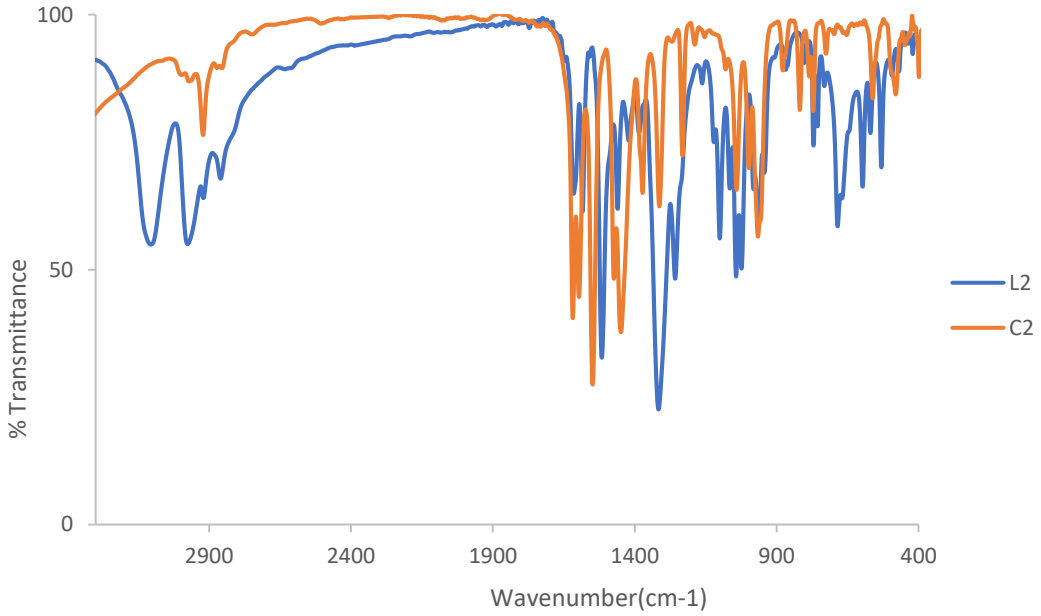

Figure C2 FTIR spectra for Schiff base ligand, **L2** and Zinc complex, **C2** in KBR.

D. ESI-MS spectra

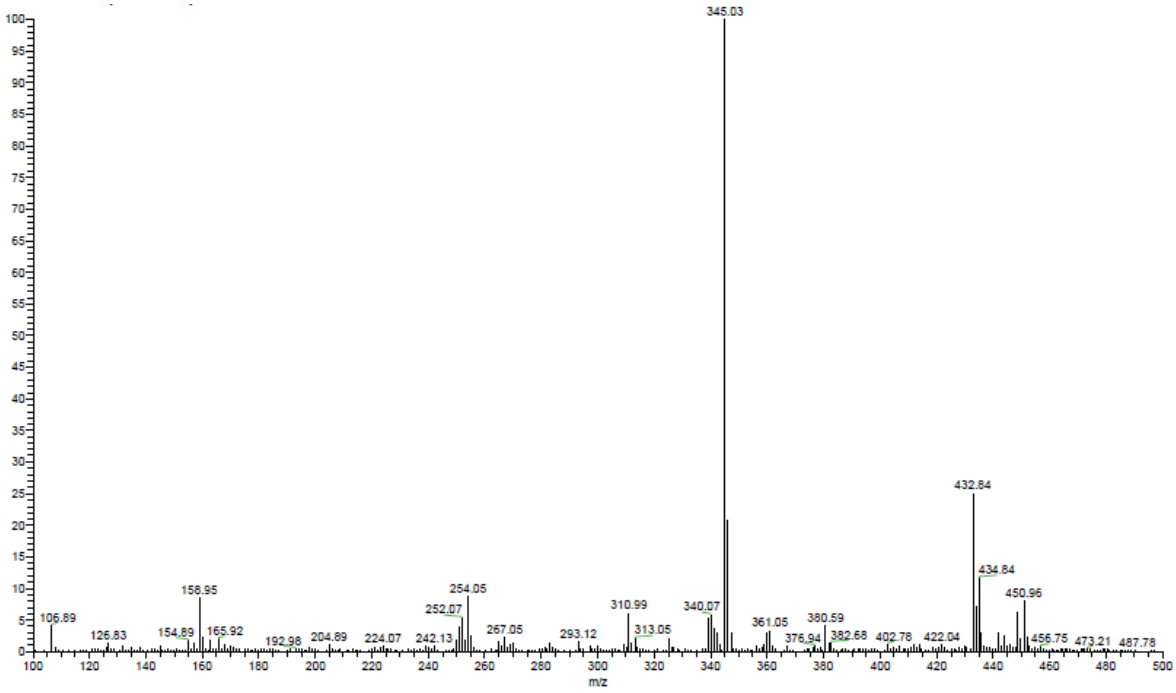

Figure D1 ESI(-) - MS spectra for **L1**.

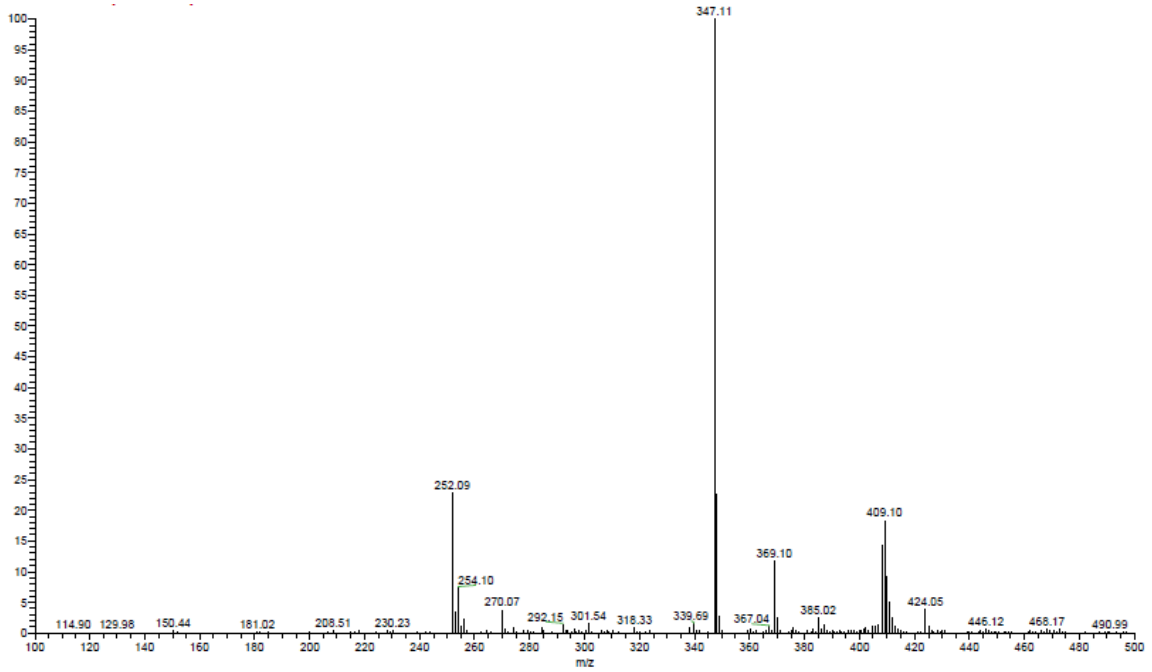

Figure D2 ESI(+) - MS spectra for **L1**.

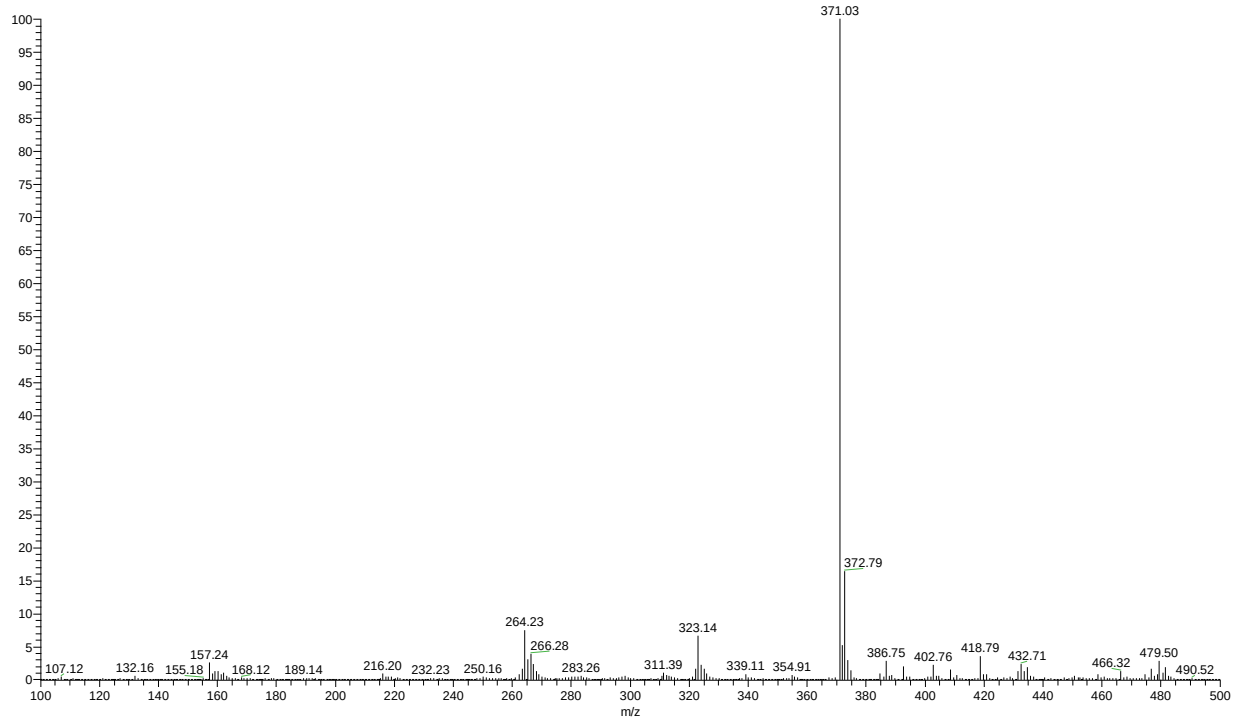

Figure D3 ESI(-) - MS spectra for **L2**.

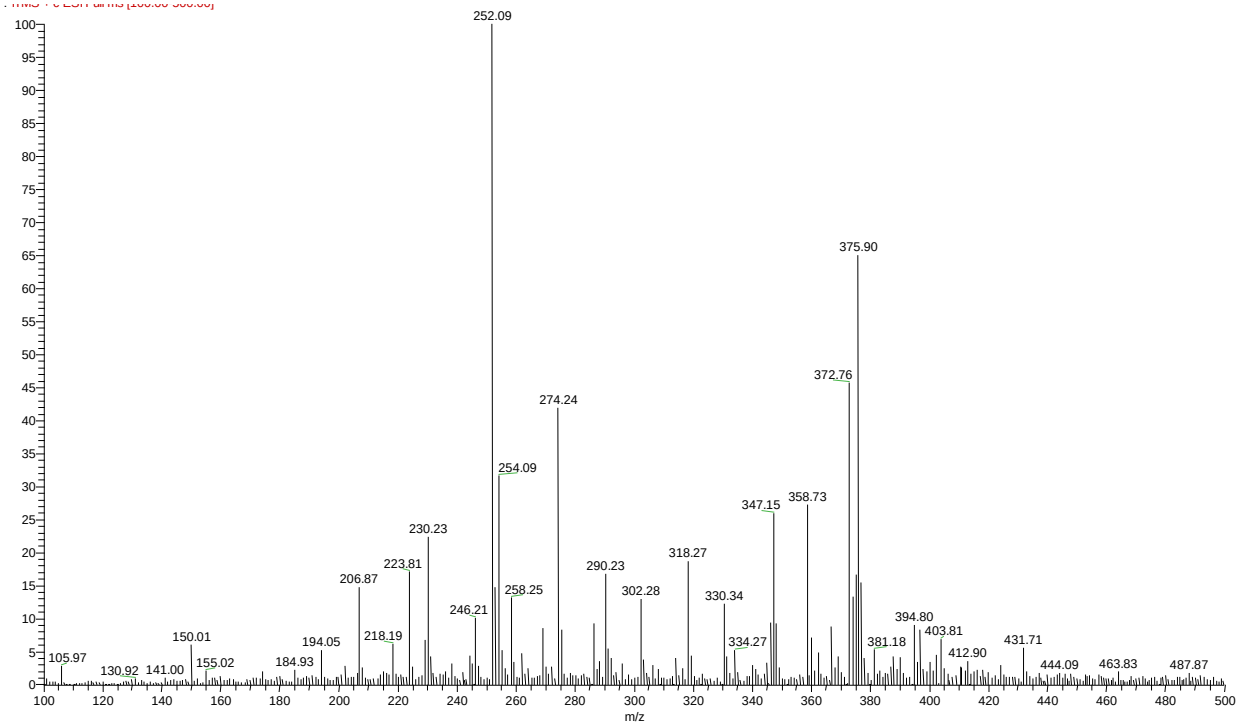

Figure D4 ESI(+) - MS spectra for **L2**.

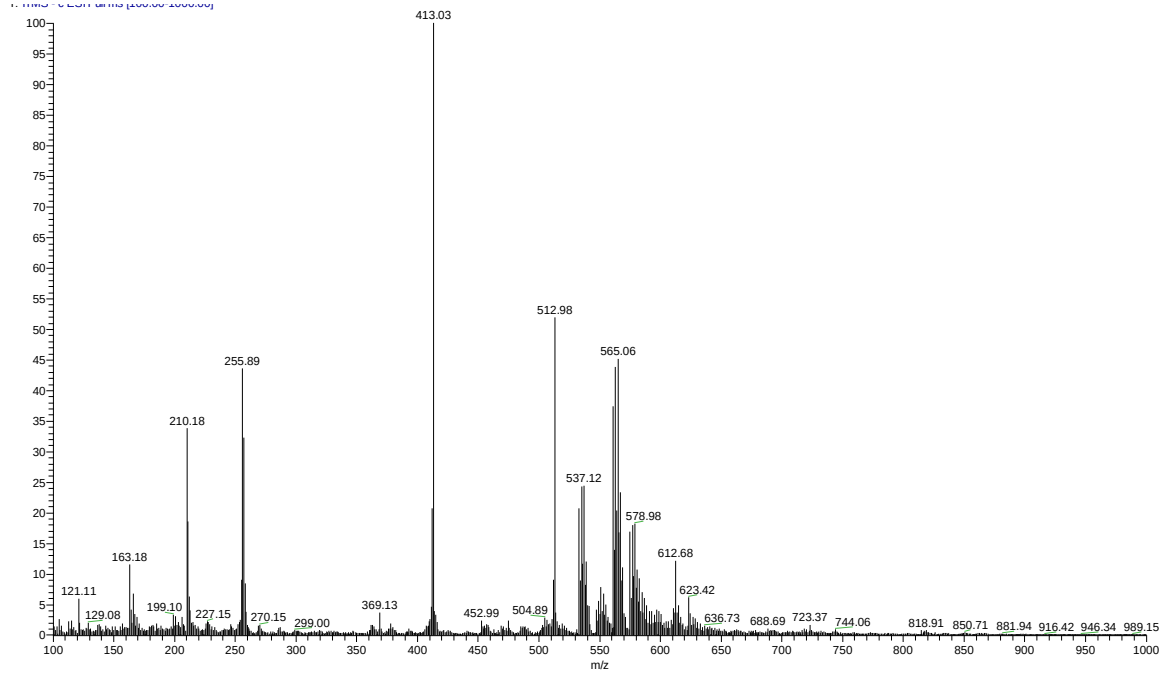

Figure D5 ESI(+) - MS spectra for **C1**.

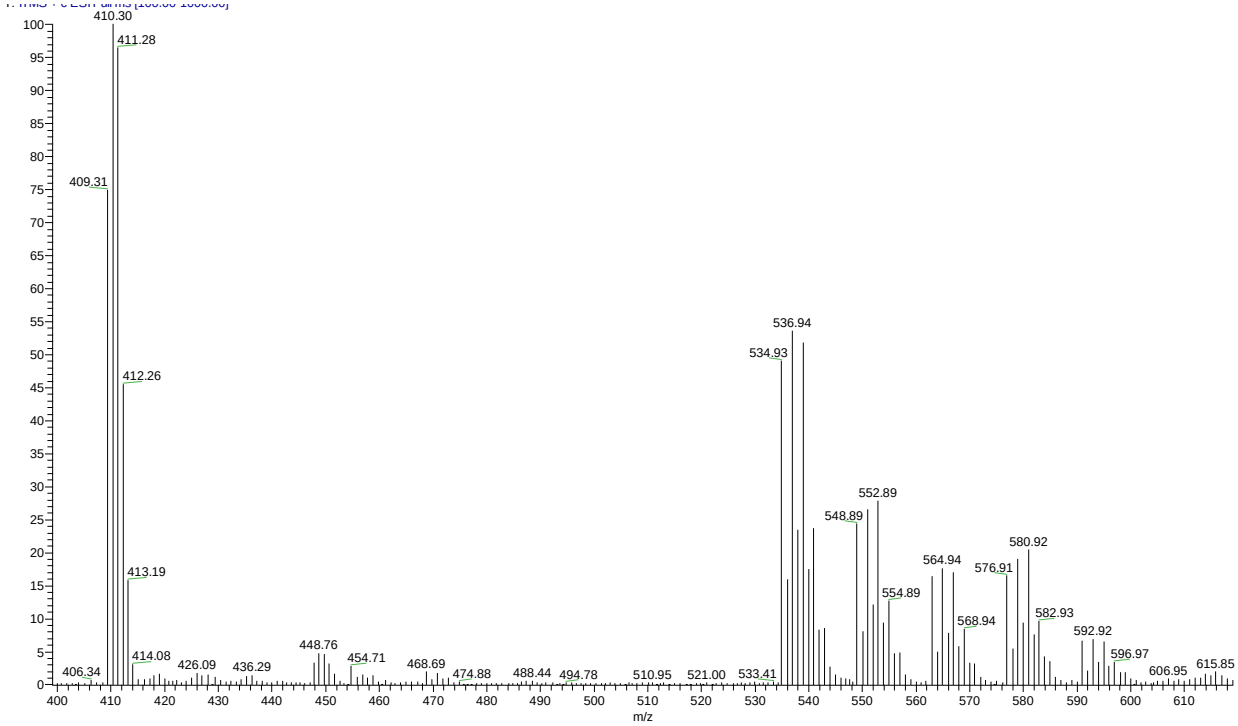

Figure D6 ESI(+) - MS spectra for **C1**.

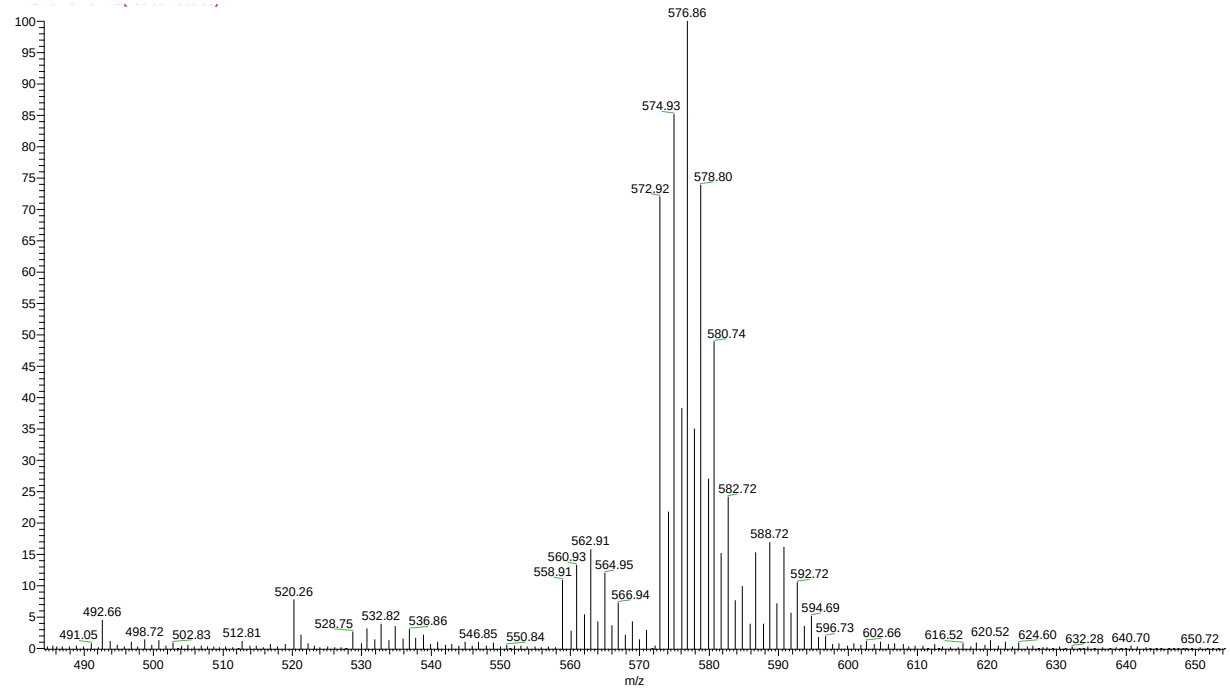

Figure D7 ESI(-) - MS spectra for **C2**.

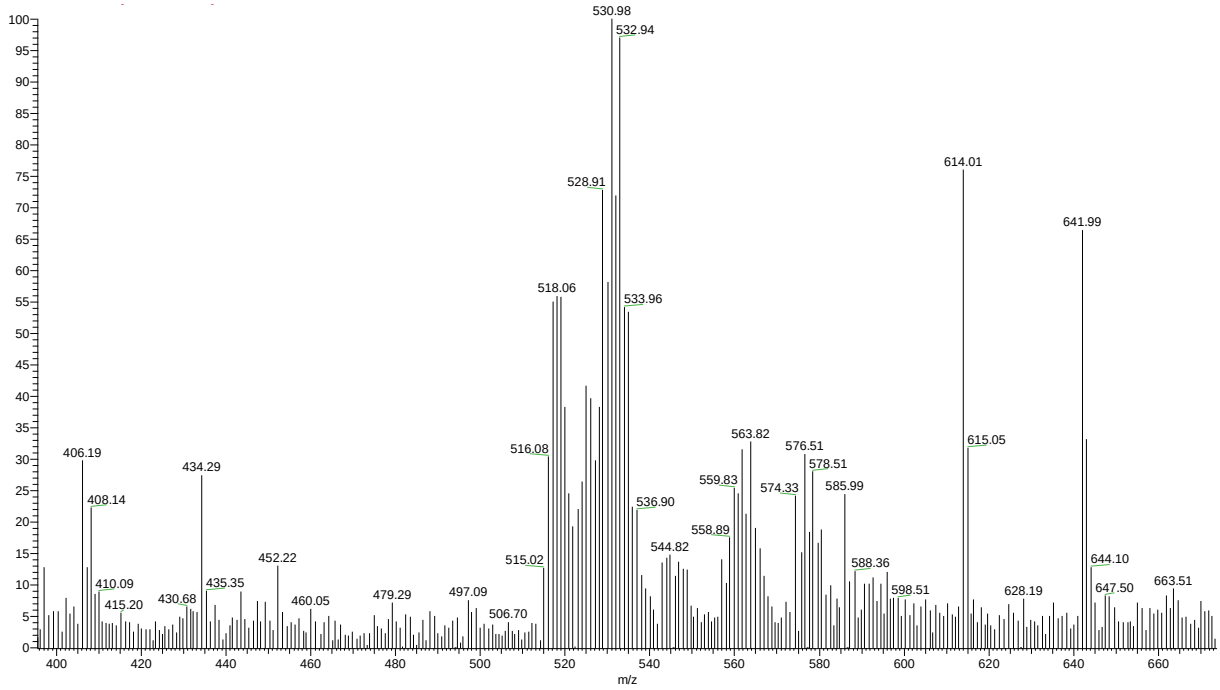

Figure D8 ESI(+) - MS spectra for **C2**.

E. Circular Dichroism spectroscopy

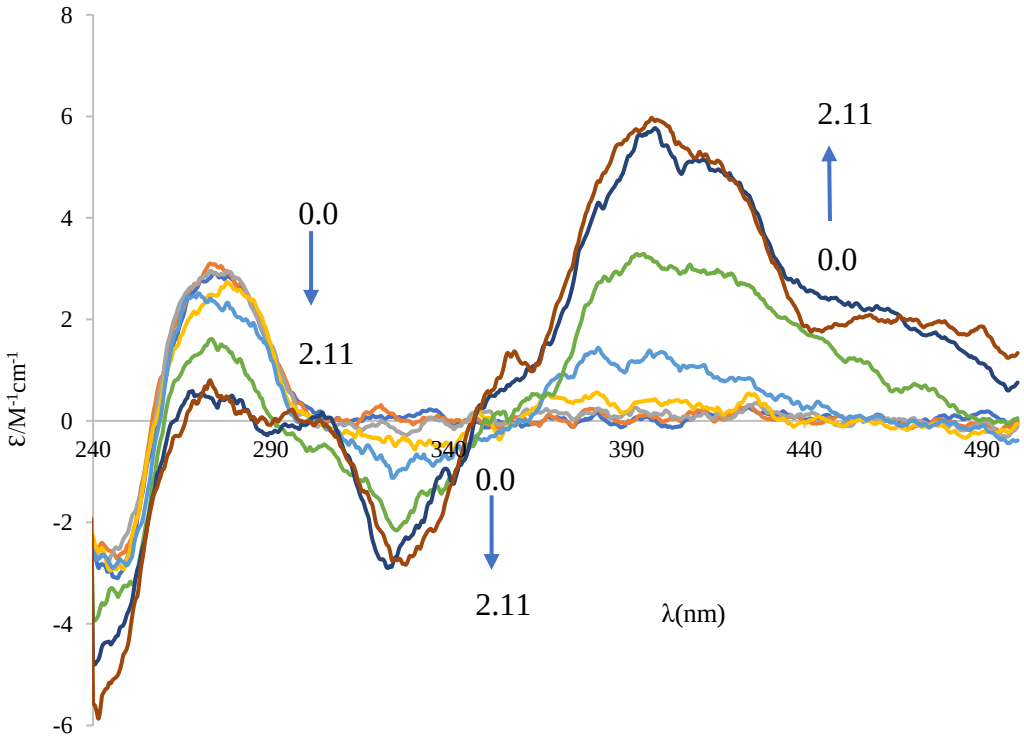

Figure E1 CD spectra for interaction of **L2** with *ct*DNA

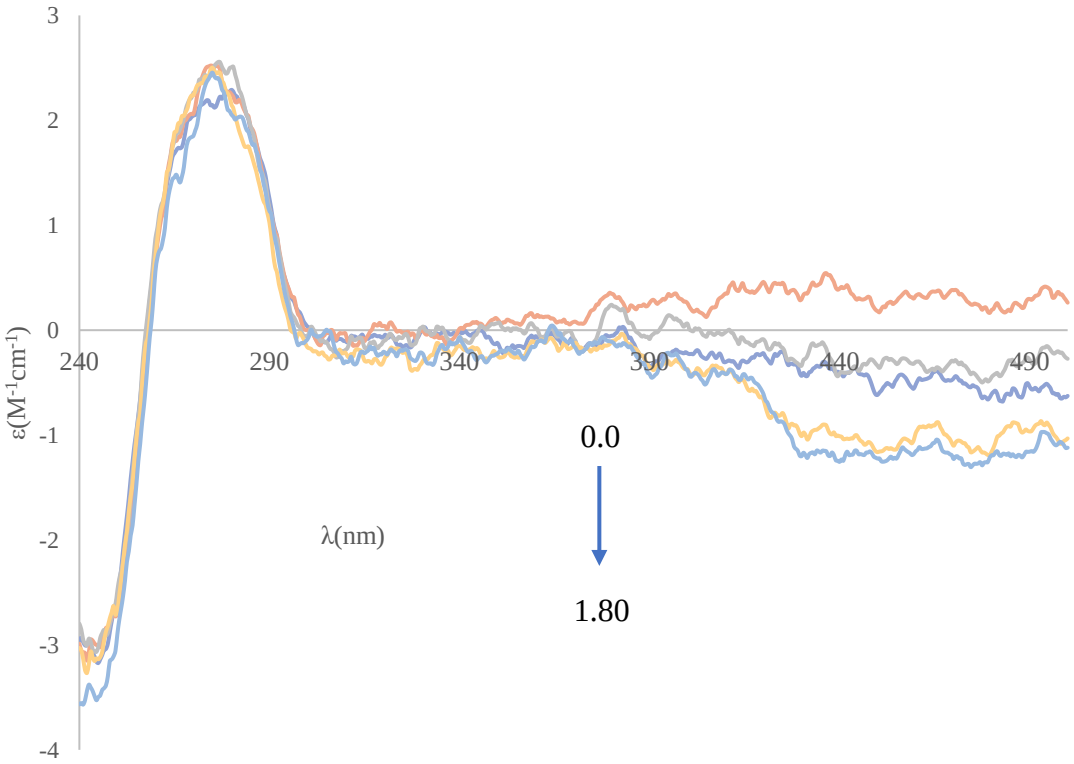

Figure E2 CD spectra for interaction of **L1** with *ct*DNA

F. UV-vis spectroscopy

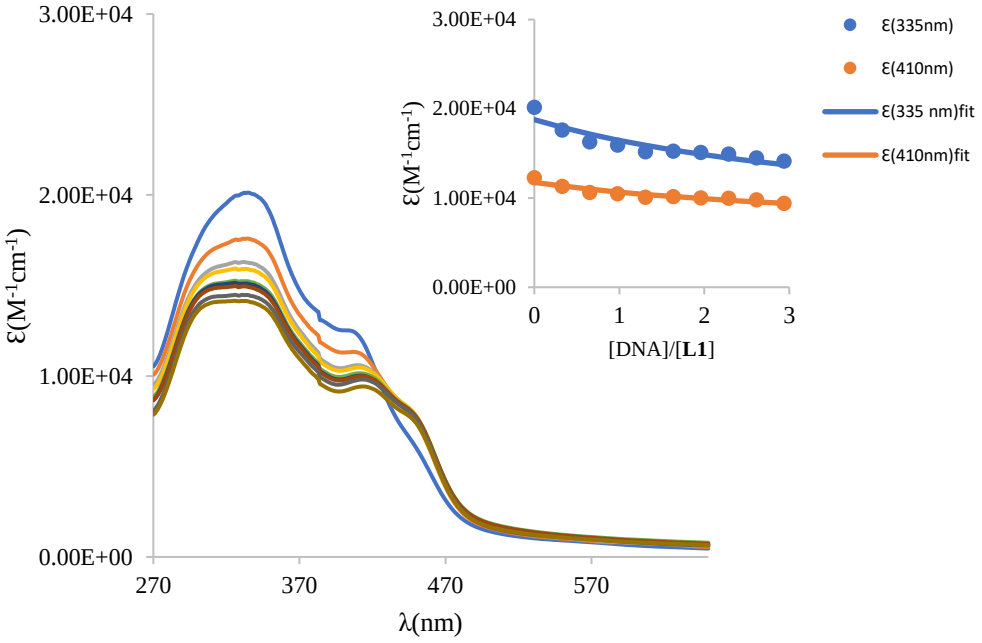

Figure F1 UV-vis spectra for interaction of **L1** with *ct*DNA

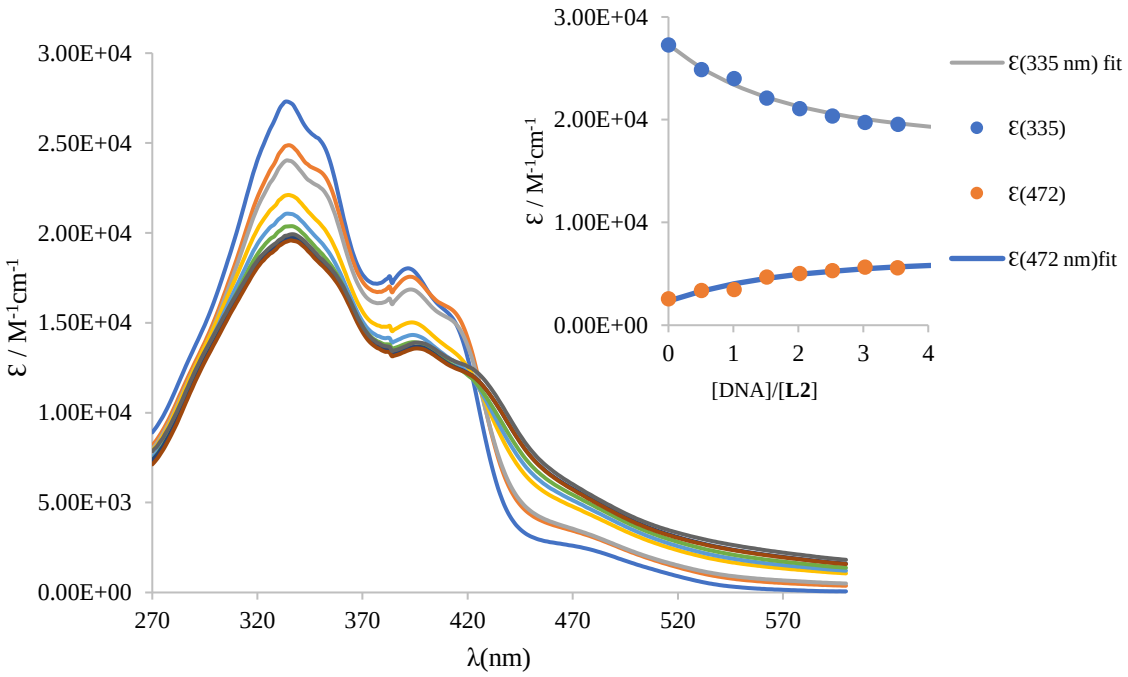

Figure F2 UV-vis spectra for interaction of **L2** with ctDNA

H. UV-vis spectra of stability studies

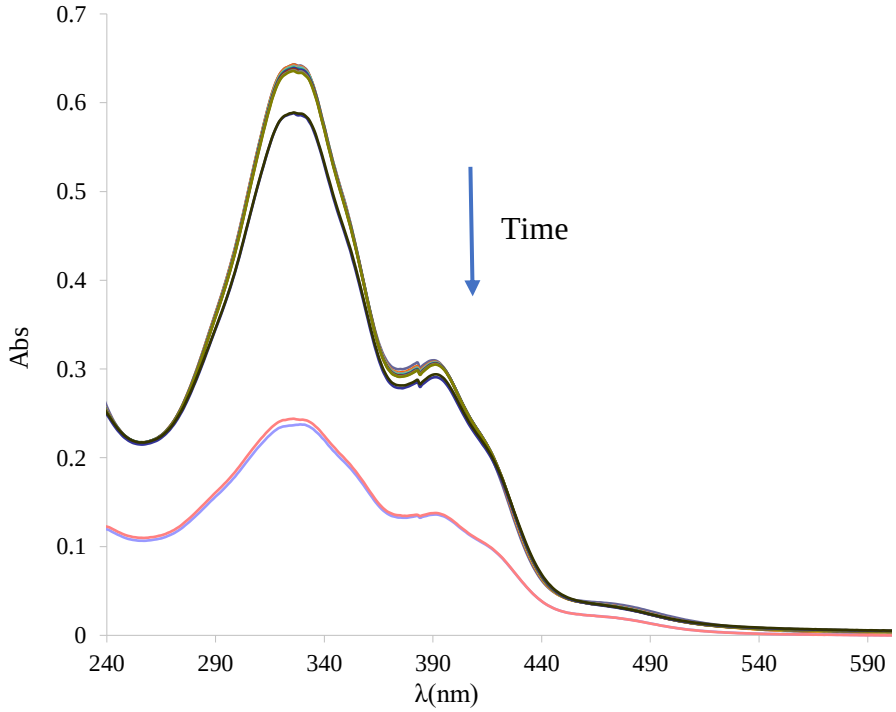

Figure H1 UV-Vis spectra for stability study of **L2** in PBS(pH 7.4, 10 mM, 25^0C)

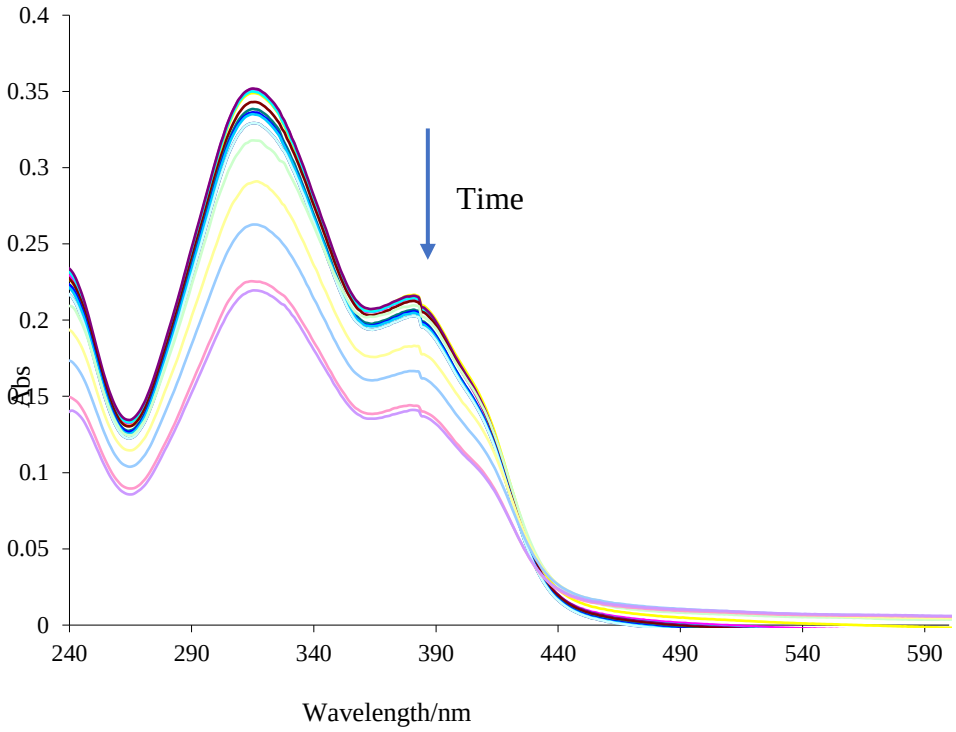

Figure H1 UV-Vis spectra for stability study of **L1** in PBS(pH 7.4, 10 mM, 25^0C)